protein that plays an important role in FGFR signaling. FRS2α binds constitutively to FGFR through its PTB domain at the NH_2 terminus and six tyrosine residues at the COOH terminus are phosphorylated by activated FGFR. Once FRS2α is phosphorylated, it recruits adaptor molecules such as Grb2 and Shp2 and relays the signals to the Ras/mitogen-activated protein kinase (MAPK) or phosphatidylinositol 3-kinase/Akt pathway (22, 23). In addition, FGFR is known to direct cytoskeletal reorganization through regulating small GTPases, although its precise signaling mechanism has not been clarified (24).

The FGF growth factor family mediates a wide range of biological activities by binding to and activating the FGFR family (25). Aberrant FGFR signaling leads to diverse human pathologies including carcinogenesis. In gliomas, malignant progression from low to high grade appears to involve up-regulation of FGFR expression (26). FGFR2 is expressed abundantly in normal white matter and in all low-grade astrocytomas but is repressed in malignant astrocytomas. Conversely, FGFR1 expression is almost absent in normal white matter but is sufficiently expressed to be detected in malignant astrocytomas (27). Glioblastomas also express an alternatively spliced form of FGFR1 containing two immunoglobulin-like disulfide loops (FGFR1β), whereas normal human adult expresses FGFR1α, a form of the receptor containing three immunoglobulin-like loops. Intermediate grades of astrocytomas exhibit a gradual loss of FGFR2 and a shift in expression from FGFR1α to FGFR1β as they progress (28). Thus, FGFR1 signaling is suggested to be associated closely with malignant progression of astrocytes.

In this article, we would like to report that our gene expression study showed aberrant expression of the EphA4 receptor in high-grade astrocytic tumors and that the overexpressed EphA4 contributed to the malignant phenotype of the tumor cells through enhancing proliferation and migration by its interaction with FGFR1.

Materials and Methods

Microarray Gene Expression Analysis

Tumor specimens were obtained from 47 patients who underwent therapeutic removal under approved protocols from the institutional review board. Histologic diagnosis was made by light microscopic evaluation of the sections stained with H&E. The classification of human brain tumors was based on the WHO criteria for tumors of the nervous system (29). The 47 brain tumors consisted of 32 high-grade glioma and 15 low-grade glioma. Total RNA was extracted from tissue samples and assessed for quality. Amplified RNA from tumor and normal brain tissue was labeled with Cy5 and Cy3 (Amersham Biosciences), respectively. Hybridization target probes were prepared from total RNA and hybridized to the CodeLink Agilent Human I Bioarray chip according to the manufacturer's instructions (Amersham Biosciences). Microarray images were processed using Gene Spring software (Silicon Genetics). Intensity values were normalized using lowess normalization (30). Average fold differences in gene expression between tumor and normal brain were calculated. Basic data visualization, data filtering, and hierarchical clustering were done. The microarray raw data and clinical features has been submitted to Gene Expression Omnibus[5] (accession no. GSE4381) in our previous report (31).

Cell Culture

GP2-293 cells (Clontech) were cultured and maintained with DMEM with 10% fetal bovine serum and used as packaging cells for pseudo-retrovirus production. RPMI 1640 supplemented with 10% fetal bovine serum was used for each culture of U251 cells (human malignant astrocytoma cell line; Japanese Collection of Research Bioresources Cell Bank).

Expression Vector Construction and Viral Production

The expression constructs of EphA4 and FGFR1 were generated as follows. The full-length cDNA fragment encoding human EphA4 or FGFR1 was obtained from the U251 cells with the reverse transcription-PCR method using the primers EphA4-P1-F (CGGATCCAC-CATGGCTGGGATTTTCTATTTC), EphA4-R (GAAGCTT-GACGGGAACCATTCTGCCGTGCATC), FGFR1-F (CGGATCCGAAATGTGGAGCTGGTGACCCCAGCA), and FGFR1-R (GAAGCTTGCGGCGTTTGAGTCCGC-CATTGGCA). The DNA fragment for EphA4 DN lacking both juxtamembrane and kinase domains was generated with the recombinant PCR method using the following primers EphA4-P1-F, EphA4-P2-R (ACTGCTTGGTTGG-GATCTTCATTCAAATGTTTCTCTTCAT), EphA4-P3-F (ATGAAGAGAAACATTTGAATGAAGATCCCAAC-CAAGCAGT), EphA4-P4-R (GAAGCTTGTTGCTGTT-CACCAGGATGTTCC). First, two DNA fragments of EphA4 were amplified using P1-F/P2-R and P3-F/P4-R primer sets. Next, the recombined DNA fragment for EphA4 DN was amplified using the two PCR products as templates and the P1-F/P4-R primer set. The DNA fragment for FGFR1 DN lacking cytoplasmic domain was amplified with the primers, FGFR1-F and FGFR1(TM)-R (CAAGCTTCTTGTAGACGATGACCGACCCCAC). The sequences of all of the PCR-amplified DNAs were confirmed by sequencing after cloning into a pCR-Blunt II-TOPO cloning vector according to the manufacturer's instructions (Invitrogen). HA and myc tag were added at the COOH-terminal ends of EphA4 and FGFR1 constructs, respectively. All DNA fragments were cut out and transferred into a pQCLIN retroviral vector (BD Biosciences Clontech) together with enhanced green fluorescent protein (EGFP) following internal ribosome entry site sequence to monitor the expression of the inserts indirectly. A pVSV-G vector (Clontech) for constitution of the viral envelope and the pQCXIX constructs were cotransfected into the GP2-293 cells using a FuGENE6 transfection reagent (Roche Diagnostics). Briefly, 80% confluent cells

[5] http://www.ncbi.nlm.nih.gov/geo

cultured on a 10 cm dish were transfected with 2 μg pVSV-G plus 6 μg pQCXIX vectors. Forty-eight hours after transfection, the culture medium was collected and the viral particles were concentrated by centrifugation at 15,000 × *g* for 3 h at 4°C. The viral pellet was resuspended in fresh RPMI 1640. The viral vector titer was calculated by counting EGFP-positive cells, which were infected by serial dilution with virus-containing medium, and the multiplicity of infection was determined. These EphA4 and FGFR1 constructs are illustrated schematically in Fig. 2A.

Antibodies and Reagents

Recombinant human FGF2 and mouse ephrin-A1/Fc chimera were purchased from R&D Systems. Antibodies used for the study were as follows: anti-MAPK rabbit polyclonal, anti-phospho-MAPK rabbit polyclonal, anti-Akt rabbit polyclonal, anti-phospho-Akt rabbit polyclonal, and horseradish peroxidase-linked second antibodies (Cell Signaling); anti-HA and anti-myc monoclonal antibodies (Roche Diagnostics); anti-FRS2 rabbit polyclonal, anti-EphA4 rabbit polyclonal, anti-FGFR1 rabbit polyclonal, and anti-RhoA mouse monoclonal (Santa Cruz); anti-phosphotyrosine mouse monoclonal and anti-Rac1 and anti-Cdc42 mouse monoclonal (BD Biosciences). Rac GTPase-specific inhibitor was purchased from Calbiochem EMD Biosciences.

Cell Proliferation Assay

Cell proliferation was assessed using a CellTiter96 Aqueous One Solution Cell Proliferation Assay kit (Promega) according to the manufacturer's instructions. Briefly, cells (1×10^3) serum-starved overnight were seeded on 96-well plastic plates with 200 μL culture medium supplemented with or without 0.5 μg/mL ephrin-A1/Fc or 20 ng/mL FGF2. After 72 h incubation at 37°C, 40 μL 3-(4,5-dimethylthiazol-2-yl)-5-(3-carboxymethoxyphenyl)-2-(4-sulfophenyl)-2H-tetrazolium, inner salt reagent was added followed by further incubation for 1 h. The absorbance at 490 nm was measured using a microplate reader.

Cell Migration Assay

The U251 cells were cultured in 12-well plates until confluence was reached. The monolayer cells were scratched out using a fine pipette tip after serum starvation overnight. To monitor the migration, pictures were taken at 0, 12, and 24 h after addition of ephrin-A1 or FGF2 using a fluorescence microscope (Keyence Biozero). The areas occupied by the cells were calculated with NIH image software (NIH). The ratio of the increased area by cell migration after 12 and 24 h to that at 0 h was calculated to quantitate the extent of migration.

Immunoblot Analysis

Cells that were serum starved for 24 h were treated with or without ephrin-A1/Fc or FGF2. The cells were washed with cold PBS and harvested with Lysis A buffer containing 50 mmol/L HEPES buffer, 1% Triton X-100, 5 mmol/L EDTA, 50 mmol/L sodium chloride, 10 mmol/L sodium pyrophosphate, 50 mmol/L sodium fluoride, 1 mmol/L sodium orthovanadate, and protease inhibitor mix, Complete (Roche Diagnostics). The lysate was clarified by centrifugation for protein analysis. The proteins separated with SDS-PAGE were transferred onto polyvinylidene difluoride membranes. After blocking with 3% bovine serum albumin in TBS (pH 8.0) with 0.1% Tween 20, the membrane was probed with the first antibody. After rinsing twice with TBS, the membrane was incubated with the horseradish peroxidase-conjugated second antibody (Cell Signaling) followed by visualization using a ECL detection system (Amersham Biosciences).

Pull-Down Assay

GTP-bound RhoA and Rac1/Cdc42 were pulled down from the cell lysate using agarose-conjugated GST-fused Rhotekin binding domain and GST-fused PAK-1 binding domain (Upstate), respectively, followed by quantitative detection by immunoblotting. Briefly, the cells were treated with or without ephrin-A1/Fc or FGF2 and lysed in magnesium-containing lysis buffer (25 mmol/L HEPES buffer, 150 mmol/L sodium chloride, 1% Triton X-100, 10% glycerol, 25 mmol/L sodium fluoride, 10 mmol/L $MgCl_2$, 1 mmol/L EDTA, 1 mmol/L sodium orthovanadate, 10 μg/mL leupeptin, and 10 μg/mL aprotinin). After clarification, an equal amount of lysate was incubated with 20 μg agarose-conjugated GST-fused Rhotekin binding domain or GST-fused PAK-1 binding domain at 4°C for 3 h. The agarose beads were washed three times with magnesium-containing lysis buffer and the samples were analyzed with SDS-PAGE followed by immunoblotting.

Immunoprecipitation

The total protein extracted with Lysis A buffer (as described above) was incubated with the antibody at 4°C overnight. The antibody was immobilized with protein A agarose by incubation for a further 2 h. The immunoprecipitates were collected by centrifugation at 3,000 × *g* for 30 s. After the immunoprecipitates were washed four times with Lysis A buffer, the samples were analyzed with SDS-PAGE followed by immunoblotting.

Statistics

Comparisons were made using Student's *t* test. $P < 0.05$ was considered statistically significant.

Results

High Expression of EphA4 mRNA in Malignant Glioma

We analyzed the expression of 13,156 clones from Incyte's human cDNA library genes using Agilent human cDNA microarrays (Agilent Technologies) for 32 malignant gliomas consisting of 10 anaplastic astrocytomas and 22 glioblastomas. We did hierarchical clustering of 103 tyrosine kinases (Fig. 1A). The histograms to determine the fold difference in the measured expression levels between tumors and normal brain are shown in Fig. 1B. Among several receptors with increased expression, we found the mRNA levels of the EphA4 receptor were significantly higher in glioma tissues (>4-fold) than those in normal brain tissues. There was a difference between anaplastic astrocytomas and glioblastomas with regard to EphA4 expression. The level in glioblastomas was higher than that in anaplastic astrocytomas. In low-grade gliomas, EphA4 expression level was also elevated but lower than

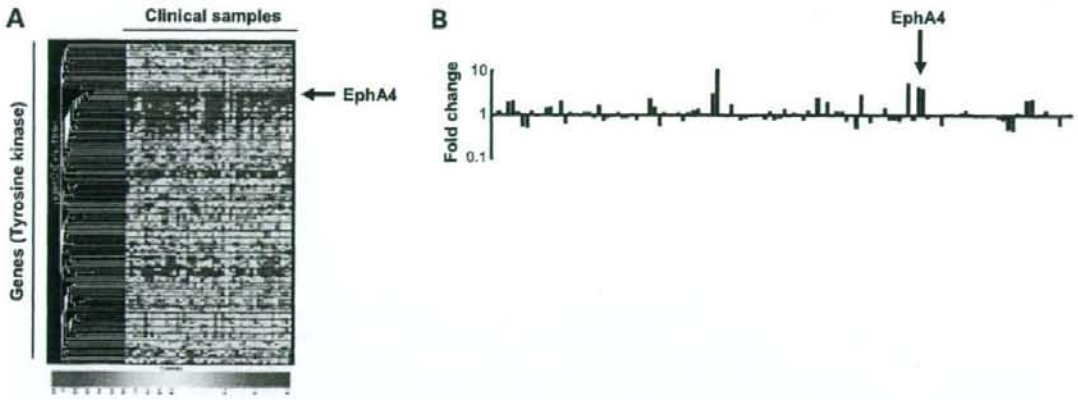

Figure 1. Profiles of 103 tyrosine kinases mRNA expression in 47 surgical samples of brain tumors. *Arrows*, EphA4 mRNA expression. **A**, hierarchical clustering of 103 tyrosine kinases. Each row and column shows a single gene and a tissue sample, respectively. The order of the clinical samples (*X axis*) corresponds to the WHO criteria from high grade to low. **B**, histogram of gene expression. The mRNA level of the EphA4 gene was significantly higher in glioma tissues (>4-fold) than in normal brain tissues.

that in high grade. EphA4 expression correlated with increasing tumor grade. The other transcripts with significantly higher expression were indicated in Supplementary Table.[6] Based on these results, we focused on the high expression level of EphA4 and examined the biological significance of EphA4 in gliomas.

Design of EphA4 and FGFR1 Constructs Used in This Study

Based on the previous evidence that EphA4 interacts with FGFR (32) and that, among the FGFR family, FGFR1 is most closely associated with the malignant progression of human glioma as described in Introduction, we sought to investigate how EphA4 affected FGFR signaling using human glioma U251 cells. For this study to explore the role of EphA4-FGFR1 interaction in glioma cell biology, it is vital to select glioma cell lines that express high levels of both EphA4 and FGFR1. However, these cell lines were not available, so we selected U251 cells, which have increased expression of FGFR1 (33), introduced EphA4 into U251 cells, and did our experiments using the transfected U251 cells.

Expression constructs of EphA4 and FGFR1 are summarized schematically in Fig. 2A. We generated a dominant-negative form of EphA4 (EphA4 DN), which lacked its juxtamembrane domain and COOH-terminal half of the kinase domain. It has been reported that EphA4 transphosphorylates FGFR through their direct interaction and that the NH_2-terminal region of the EphA4 kinase is necessary to interact with the FGFR (32). The juxtamembrane domain is postulated to close its interaction portion constitutively when EphA4 kinase is inactive. Therefore, this juxtamembrane-deleted EphA4 mutant can expose its binding site to FGFR although lacking transphosphorylation activity. In addition, this kinase-inactive mutant can also work as an EphA4 inhibitor against ephrin-ligand stimulation. On the contrary, a dominant-negative form of FGFR1 (FGFR1 DN) lacks the whole cytoplasmic domain, which inhibits the activation of intrinsic FGFR1 by FGF stimulation. These wild-type and dominant-negative constructs of both EphA4 and FGFR1 were retrovirally introduced into human glioma U251 cells and their protein expression was checked as seen in Fig. 2B. As the expression unit included an internal ribosomal entry site sequence followed by EGFP, we could monitor the expression by fluorescence microscopy in Fig. 2C.

EphA4 Promotes FGF2-Mediated Proliferation and Enhances FRS2, MAPK, and Akt Phosphorylation in U251 Cells

We evaluated the effect of EphA4 on cell proliferation of the U251 cells using the ectopic expression of EphA4 WT retrovirally. EphA4 WT did not affect cell proliferation significantly without FGF stimulation but promoted cell proliferation significantly in the presence of FGF2 at 20 ng/mL for 72 h compared with a mock control (Fig. 3A). Inversely, EphA4 DN expression as well as FGFR1 DN inhibited FGF2-triggered proliferation. FGF2-triggered proliferation of FGFR1 DN was higher than that with no ligand stimulation. The reason might be that FGFR1 DN could not completely block FGF2-mediated FGFR1 activation. However, FGF2-induced cellular responses were clearly inhibited in FGFR1 DN compared with those in the other cells. Ephrin-A1 stimulation seemed slightly to promote cell proliferation for EphA4 WT cells, FGFR1 DN-expressing cells, and mock control cells, but it was not statistically significant. These results suggested some strong correlation of EphA4 with FGFR signaling.

[6] Supplementary materials for this article are available at Molecular Cancer Therapeutics Online (http://mct.aacrjournals.org/).

Then, we sought to examine whether downstream signals of the FGFR were modulated by overexpression of EphA4. First, we checked the phosphorylation level of FRS2, which was well known to relay the FGFR signals via its tyrosine phosphorylation. FRS2 phosphorylation by FGF2 stimulation was detectable in the mock control cells as shown in Fig. 3B. In EphA4 WT-introduced U251 cells, the FGF2-induced phosphorylation was more evident. Inversely, EphA4 DN, as well as FGFR1 DN, weakened FRS2 phosphorylation compared with the mock control cells. It was unlikely that EphA4 promoted FRS2 phosphorylation directly because ephrin-A1 stimulation itself did not induce FRS2 phosphorylation in any cells. This promotive effect of EphA4 on FRS2 phosphorylation was considered to occur possibly through activated FGFR following FGF2 stimulation.

Next, we checked the phosphorylation levels of MAPK and Akt, which were well known to affect cell proliferation and survival, respectively. Those were further downstream signaling molecules of FGFR and were also relayed via FRS2 phosphorylation. From time-course analysis of phosphorylated MAPK and Akt stimulated by 20 ng/mL FGF2, we found that their phosphorylation level reached a peak at around 15 min. Although MAPK was not phosphorylated by Ephrin-A1 stimulation, Akt-phosphorylation was clear and peaked at 30 min (data not shown). We therefore selected 15 and 30 min to evaluate the degree of MAPK and Akt phosphorylation by FGF2 and ephrin-A1, respectively. Phosphorylated MAPK and Akt and their total proteins are shown in Fig. 3C (*left* and *right*, respectively). FGF2 stimulation clearly phosphorylated MAPK and Akt; especially, EphA4 WT augmented FGF2-induced phosphorylation of MAPK and Akt compared with the mock control cells (Fig. 3D). On the contrary, EphA4 DN as well as FGFR1 DN attenuated FGF2-mediated MAPK and Akt phosphorylation. Notably, the baseline phosphorylation levels of both MAPK and Akt were moreover increased in the EphA4 WT-introduced U251 cells without ligand stimulation but inhibited in the EphA4 DN-introduced cells. Ephrin-A1 stimulation showed an almost undetectable increase of phospho-MAPK but a small increase of phospho-Akt. EphA4 DN

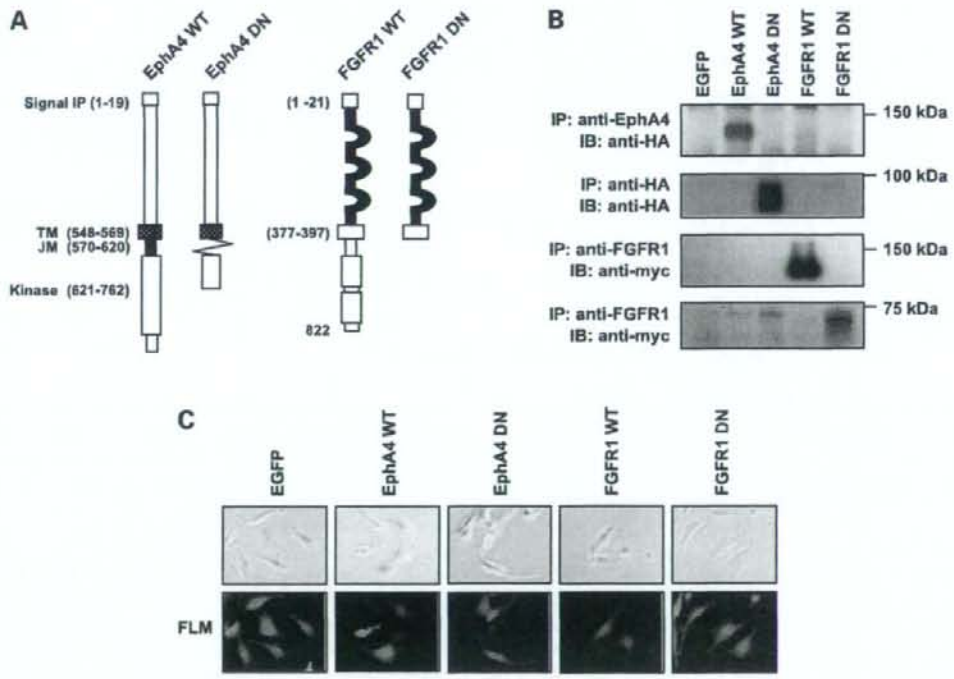

Figure 2. Construction of expression vectors for either the wild-type (*WT*) or the dominant-negative (*DN*) form of EphA4 or FGFR1. **A**, schematic representation of EphA4 and FGFR1 constructs. *Numbers*, amino acids. EphA4 DN is a deletion mutant lacking the juxtamembrane (570-620) and COOH-terminal half of EphA4 kinase domain (763-986) amino acids. FGFR1 DN is also a deletion mutant without whole cytoplasmic domain. *TM*, transmembrane domain; *JM*, juxtamembrane domain. **B**, checking the expression of EphA4 and FGFR1 constructs in U251 cells. EphA4 and FGFR1 constructs were tagged with HA and myc, respectively, at the COOH terminus. Each lysate (500 μg) was immunoprecipitated and detected by immunoblotting with the HA or myc antibody. *IB*, immunoblotting; *IP*, immunoprecipitation. **C**, microscopic imaging of EGFP coexpressing with the introduced proteins of interest. *FM*, fluorescent microscopy.

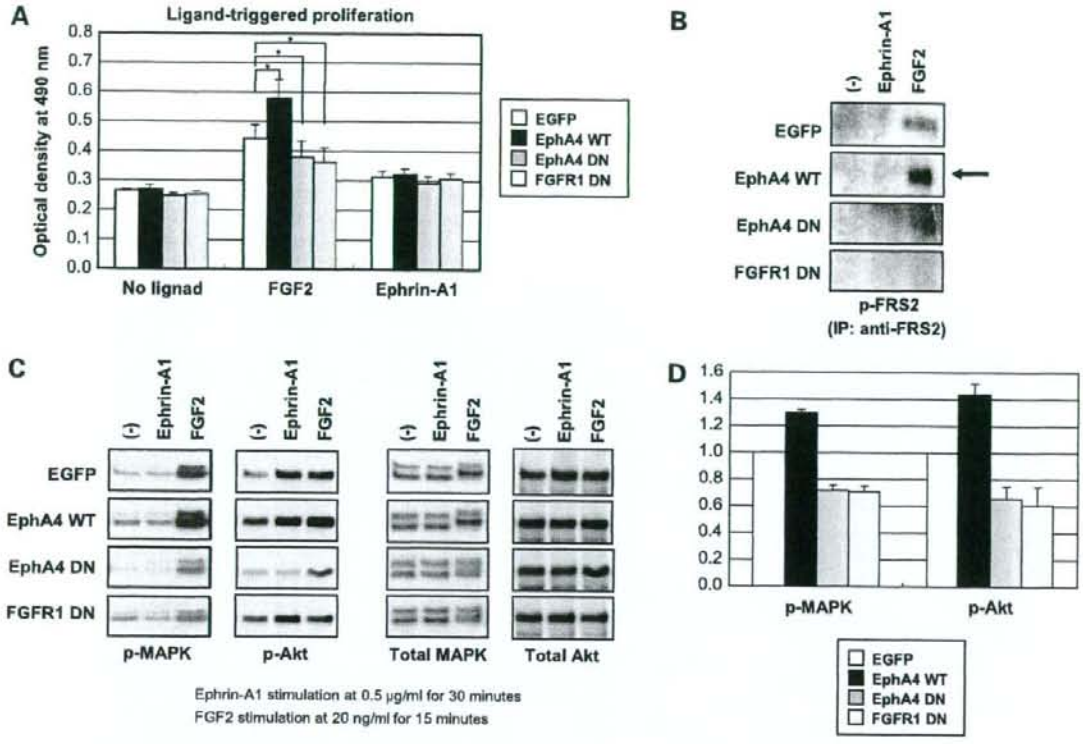

Figure 3. Effects of EphA4 WT on proliferation in the U251 cells. **A,** cell proliferation judged by the 3-(4,5-dimethylthiazol-2-yl)-5-(3-carboxymethoxyphenyl)-2-(4-sulfophenyl)-2H-tetrazolium, inner salt assay. Serum-starved cells (1×10^3) were plated on 96-well plates in the absence or presence of ligands (20 ng/mL FGF2 or 0.5 μg/mL ephrin-A1). The absorbance at 490 nm of each well was measured after 72 h incubation. *Bars,* SD. *, $P < 0.05$ versus the EGFP cells. **B,** effect of EphA4 on FRS2 phosphorylation. Serum-starved cells were treated with 20 ng/mL FGF2 for 15 min or 0.5 μg/mL ephrin-A1 for 30 min. The immunoprecipitated samples using an anti-FRS2 antibody were checked by immunoblotting with an anti-phosphotyrosine antibody. **C,** effect of EphA4 on phosphorylation of MAPK and Akt. Each cell lysate (10 μg) treated with 20 ng/mL FGF2 for 15 min or 0.5 μg/mL ephrin-A1 for 30 min was analyzed by immunoblotting. *Left,* probing with anti-phospho-MAPK and anti-phospho-Akt antibodies; *right,* reprobing with anti-total MAPK and anti-total Akt antibodies. **D,** relative densitometric units of the phospho-MAPK and phospho-Akt bands in each cell stimulated by FGF2. The densities of the EGFP bands are set arbitrarily at 1.0. *Bars,* SD.

blocked this increase, but FGFR1 DN did not, suggesting that ephrin-A1-triggered Akt phosphorylation was not mediated by FGFR1.

EphA4 Also Promotes FGF2-Mediated Migration Accompanied with Increased Active Rac1/Cdc42

To study the effect of EphA4 on cell migration, we did a scratch wound assay using the U251 cells ectopically expressing EGFP, EphA4 WT, EphA4 DN, or FGFR DN and checked the extent of their migration after scratching by monitoring EGFP for 24 h (Fig. 4A). If the incubation time is so long that migrating cells are able to proliferate, the migration rate could be affected by proliferation. Therefore, we analyzed the migration rate before proliferation might have a significant effect on this analysis (Fig. 4B). It was evident that EphA4 WT promoted FGF2-stimulated cell migration to cover the scratched area compared with the mock control and EphA4 DN (Fig. 4A, *top*). Under the same experimental condition, FGF2 stimulation caused a small increase in cell proliferation and the difference of proliferation was quite limited among the transfected cells (Supplementary Fig. S1).[6] These results imply that the wound closing process is due to cell migration activity triggered by FGF2. To evaluate this quantitatively, we assayed in triplicate and calculated the migration area (by square inches) using NIH imaging software and illustrated this graphically (Fig. 4B, *top*). EphA4 WT-expressing cells significantly migrated more than EGFP-expressing, EphA4 DN-expressing, or FGFR1 DN-expressing cells for 24 h. Interestingly, the promotion of cell migration by EphA4 WT was also observed under ephrin-A1 stimulation (Fig. 4A, *bottom*). As for ephrin-A1 treatment, cell proliferation was slightly induced in the transfected cells (Fig. 3A). Therefore, promoted wound closure means increased activity of cell migration triggered by ephrin-A1.

As Rho family GTPases have been known to play key roles in cell migration by regulating actin dynamics, we

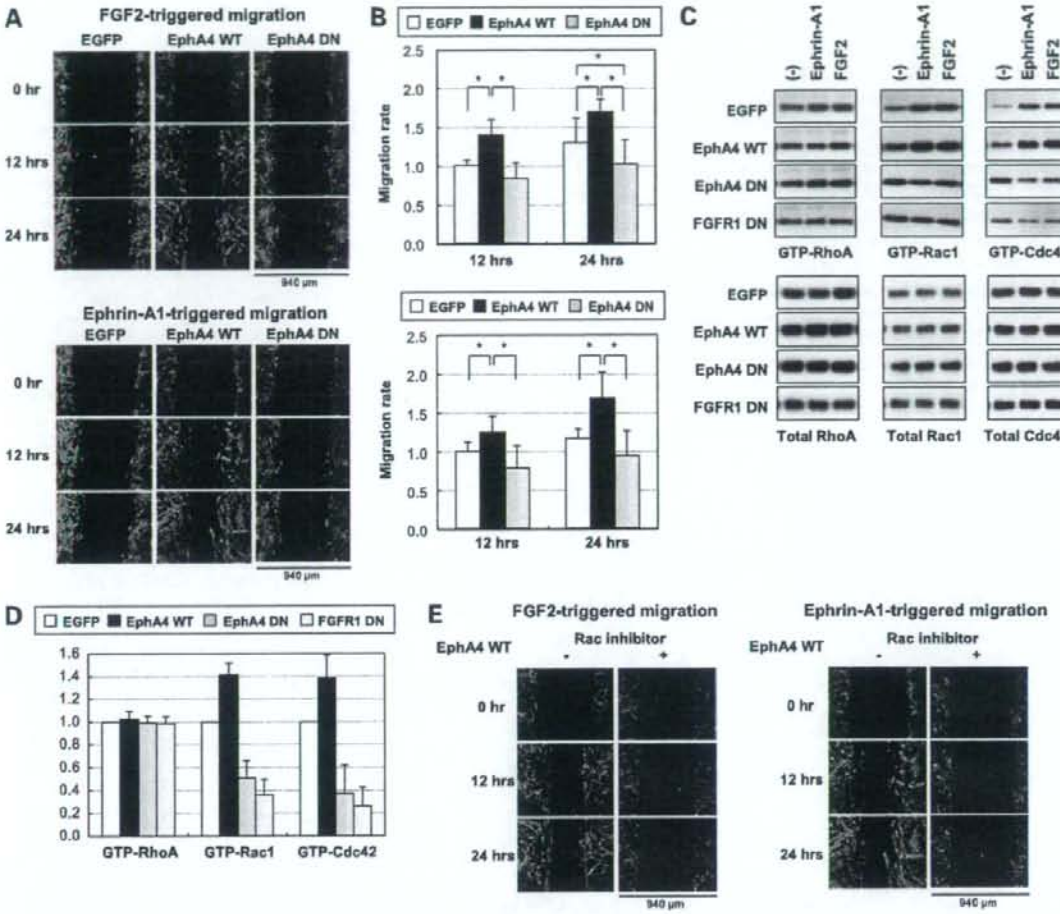

Figure 4. Effect of EphA4 WT on migration in the U251 cells. **A**, evaluation of cell migration by scratch wound assay. Serum-starved cells were cultured in the presence of 20 ng/mL FGF2 (*top*) or 0.5 μg/mL ephrin-A1 (*bottom*). The degree of migration was checked by monitoring EGFP. Pictures were shown at 12 and 24 h after ligand stimulation. **B**, extent of cell migration was quantified and shown graphically (*right*). The areas occupied by the cells were calculated with NIH image software. The ratio of the increased area after 12 and 24 h to that at 0 h was then calculated to quantitate the extent of migration. *Bars*, SD. *, $P < 0.05$ versus the EGFP cells. **C**, effects on activation of Rho GTPases. *Top*, active RhoA, Rac1, and Cdc42 of each cell stimulated by 20 ng/mL FGF2 for 15 min or 0.5 μg/mL ephrin-A1 for 30 min. The active Rho GTPases were pulled down as described in Materials and Methods and checked by immunoblotting using the indicated antibodies. *Bottom*, protein expression of three Rho GTPases using whole protein lysate. **D**, relative densitometric units of the GTP-RhoA, Rac1, and Cdc42 bands in each cell stimulated by FGF2. The densities of the EGFP bands are set arbitrarily at 1.0. *Bars*, SD. **E**, effect of Rac inhibitor on ligand-triggered migration in the transfected U251 cells of EphA4 WT. Cell migration was evaluated by scratch wound assay. Serum-starved cells were cultured in the presence of 20 ng/mL FGF2 (*left*) or 0.5 μg/mL ephrin-A1 (*right*) plus 50 μmol/L Rac inhibitor. The degree of migration was checked by monitoring EGFP. Pictures were shown at 0, 12, and 24 h after stimulation.

sought to examine how the activity of Rho GTPases would be affected by EphA4. Rho GTPase activities were evaluated by immunoblotting following a pull-down assay. FGF2 stimulation activated Rac1/Cdc42 as shown in Fig. 4B. EphA4 WT promoted activation of Rac1/Cdc42 stimulated by FGF2, whereas EphA4 DN, as well as FGFR1 DN, inhibited their activation, suggesting EphA4 promotes FGF2-mediated activation of Rac1/ Cdc42. Similarly, Rac1/Cdc42 activities stimulated by ephrin-A1 were also promoted by EphA4 WT but were inhibited by EphA4 DN, suggesting EphA4 promotes ephrin-A1-mediated activation. Importantly, the activation was inhibited by FGFR1 DN. As shown in Fig. 3A, ephrin-A1 did not induce FRS2 phosphorylation; therefore, it was suggested that the effect of EphA4 WT on ephrin-A1-triggered activation of Rac1/Cdc42 was, at least in part, through FGFR-mediated

signaling not involving FRS2. Consistent with these results, cotreatment of Rac inhibitor with FGF2 or ephrin-A1 drastically inhibited the wound closure in the scratch wound assay (Fig. 4E), showing that Rac inhibition blocked FGF2- or ephrin-A1-triggered glioma cell migration. On the other hand, neither ephrin-A1 nor FGF2 stimulation induced any RhoA activity in EGFP-expressing mock control cells and the activity was not modulated by EphA4 WT, EphA4 DN, or FGFR1 DN. These results suggest that EphA4 enhances FGF2-induced activation of Rac1/Cdc42 and promotes glioma cell migration.

EphA4-FGFR1 Heteroreceptor Complex Enhances FGF2-Triggered Phosphorylation of FGFR1

Based on the results that EphA4 promoted FGF2-mediated cell proliferation and migration as we have shown thus far, we hypothesized a functional relationship between EphA4 and FGFR1, which would affect FGFR1 activity. First, we checked their physiologic interaction by the ectopic expression of EphA4 WT and/or FGFR1 WT retrovirally using the U251 cells. FGFR1 was not detected to be coimmunoprecipitated with EphA4 in EGFP-expressing control cells (Fig. 5A). When stimulated by Ephrin-A1, coimmunoprecipitation of FGFR1 was detectable in EphA4 WT- or FGFR1-expressing U251 cells. This complex formation was most evident in EphA4- and FGFR1-coexpressing cells, meaning that activated EphA4 prefers to forming a receptor complex with FGFR1 in the U251 cells.

To clarify the functional effect of EphA4 on FGFR1 activation, we next examined the tyrosine phosphorylation level of FGFR1 in the U251 cells (Fig. 5B). Without FGF2 stimulation, neither EphA4 WT, EphA4 DN, nor FGFR1 DN affected the phosphorylation level of intrinsic FGFR1. FGFR1 was naturally phosphorylated by FGF2 stimulation in EGFP-expressing cells. This phosphorylation was further enhanced by EphA4 WT. Contrarily, EphA4 DN or FGFR1 DN inhibited FGFR1 phosphorylation by FGF2, revealing that EphA4 strengthened FGF2-mediated phosphorylation of FGFR1. Under this experimental condition, EphA4 was weakly phosphorylated by exogenous addition of FGF2 (Supplementary Fig. S3).[6] These results showed that EphA4 enhanced FGF2-triggered activation of FGFR1 through a EphA4-FGFR1 heteroreceptor complex, which possibly explained the reason that EphA4 promoted downstream signaling of FGFR and contributed to glioma cell proliferation and migration. On the other hand, ephrin-A1 stimulation did not lead to enhanced phosphorylation of FGFR1 in this experimental condition, although EphA4 was clearly phosphorylated by ephrin-A1 (Supplementary Fig. S2).[6] This might, in part, correlate to the result that FRS2 was phosphorylated by FGF2 not by ephrin-A1 (Fig. 3B).

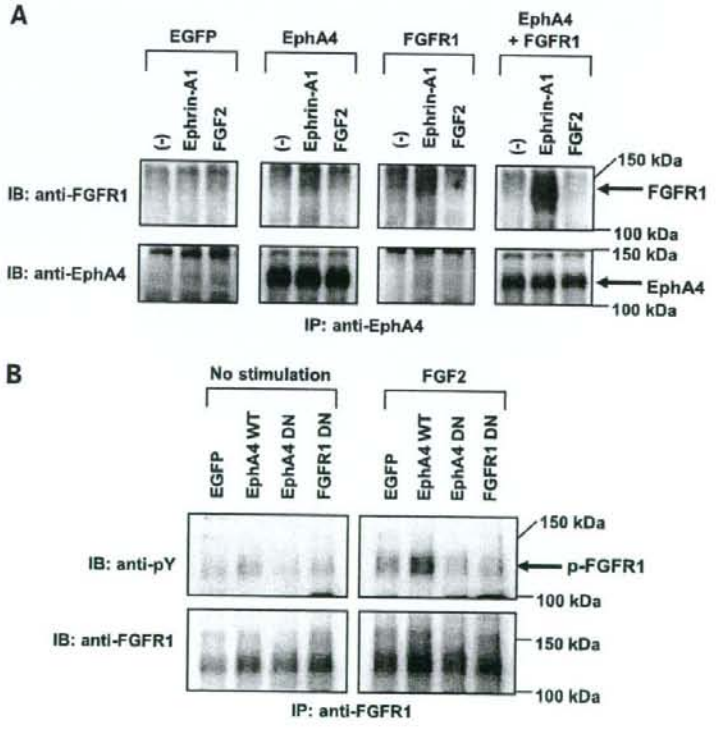

Figure 5. EphA4-FGFR1 interaction. **A**, EphA4 forms a protein complex with FGFR1. The U251 cells coexpressing EphA4 and FGFR1 were used in addition to those expressing EGFP, EphA4, and FGFR1. *Top*, EphA4 protein was immunoprecipitated from the cell lysate treated with or without 0.5 μg/mL ephrin-A1 for 30 min (ephrin-A1) or 20 ng/mL FGF2 for 15 min (FGF2) and separated by SDS-PAGE followed by immunoblotting using an anti-FGFR1 antibody. *Bottom*, reprobing with an anti-EphA4 antibody. **B**, enhanced phosphorylation of FGFR1 by EphA4. Each cell was treated with or without 40 ng/mL FGF2 for 15 min (FGF2) and the tyrosine phosphorylation level of FGFR1 was examined by probing using an anti-phosphotyrosine antibody (*top*). The total levels of precipitated FGFR1 were detected by reprobing with an anti-FGFR1 antibody (*bottom*).

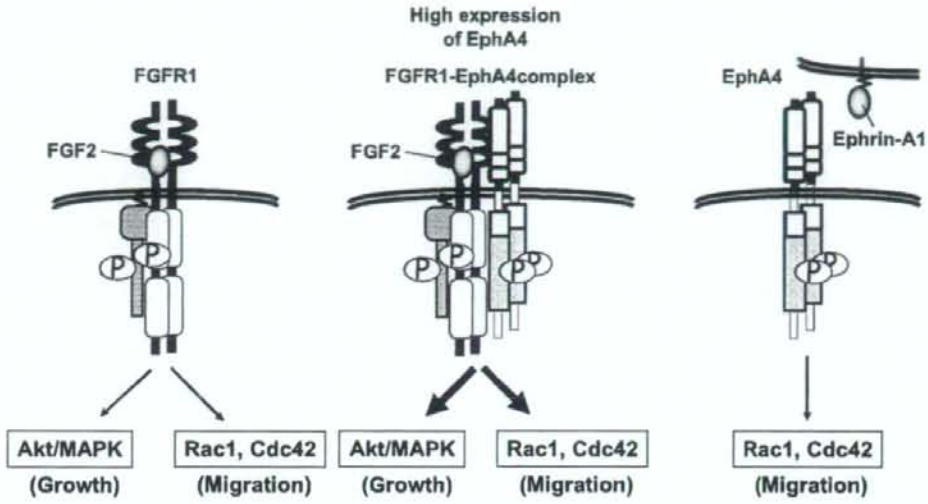

Figure 6. A diagram of the proposed mechanism of enhanced FGFR signaling by EphA4 overexpression.

Discussion

Our study revealed that highly expressed EphA4 in malignant gliomas functions as an accelerator of glioma cell proliferation and migration through promoting the FGFR1 signaling pathway as summarized in Fig. 6, suggesting that EphA4 might be a potential therapeutic target for malignant glioma.

Our microarray gene expression analysis for 32 surgical specimens of high-grade astrocytomas showed that EphA4 mRNA was expressed 4-fold higher in tumors than in normal brain tissue. Elevated expression of Eph members has been described in various human cancers (18). EphA4 expression has also been reported in cancers such as prostate, colon, and melanoma, although it has never been described in association with malignant gliomas. Among the Eph receptor family, EphA2, EphA5, and EphB2 expression has been described previously in glioblastoma cells (20, 34–36). Bruce et al. have identified aberrant EphA5 expression and showed that activation of EphA5 does not promote cell proliferation in glioma cell line (34). Nakada et al. reported phosphorylation of R-Ras associated with EphB2 effects on glioma cell adhesion, growth, and invasion (20, 35). Recently, EphA2 elevated in glioblastoma multiforme stimulated by ephrin-A1 was reported to induce an inhibitory effect on the growth and invasiveness of glioblastoma multiforme cells (36). As shown in Fig. 4A and *B* (*bottom*), the promotion of cell migration by EphA4 WT was observed under ephrin-A1 stimulation. Correspondingly, Rac1/Cdc42 activities stimulated by ephrin-A1 were promoted by EphA4 WT (Fig. 4C and *D*). Although, to the best of our knowledge, EphA4 has never been reported about glioma cell motility, these results suggest that ephrin-A1-triggered activation of EphA4 enhances Rac1/Cdc42 activation and promotes glioma cell migration (Fig. 6).

Recently, Nakada et al. revealed that ephrin-B3 promotes glioma invasion using U251 that is a high expressor cell line of ephrin-B3 and that knockdown of ephrin-B3 in U251 resulted in morphologic change and decreased migration and invasion induced by EphB2 (37). Although, in this article, EphA4 was not discussed in association with ephrin-B3, there are some previous reports about the interaction between ephrin-B3 and EphA4 (38, 39). In summary, these studies provide the evidence that EphrinB3/EphA4 has an important role in neuronal circuit formation, growth, and development. Based on this information, there is a possibility that the interaction between ephrin-B3 and EphA4 plays some role in the malignant phenotype of cancer. However, as shown in Supplementary Fig. S2A,[6] EphA4 was not phosphorylated even in the EphA4-overexpressing U251 cells without ligand stimulation, although ectopically expressing EphA4 could be activated by endogenous ephrin-B3. There was no significant difference between the mock control and the EphA4-overexpressing cells without ligand stimulation in glioma cell proliferation and migration (Figs. 3A and 4A). Together with these data, the interaction between endogenous ephrin-B3 and EphA4 did not appear to affect the results in our experimental condition.

The MAPK pathway is well known to play a major role in the tumor cell proliferation (40). There are several reports regarding the regulation of this pathway by Eph signaling (6). However, some studies report negative regulation of MAPK pathway by Eph receptor activation (41–43). Reversely, others show positive regulation of the pathway by Eph signaling, although the precise mechanism has not

been shown (44–46). In addition, Yokote et al. reported a positive-regulating mechanism of the MAPK pathway by EphA4 through direct interaction with the FGFR receptor and its activation (32). Our report also showed that FGFR1 signaling was enhanced by EphA4 through their interaction followed by an increased MAPK pathway in the U251 glioma cells. Corresponding to the increased MAPK, proliferation of glioma cells was also promoted by EphA4. It was important that this enhancement was dependent on FRS2 phosphorylation, which was suggested by the findings that either FGFR1 DN or EphA4 DN inhibited FRS2-MAPK signaling enhanced by EphA4. In addition, it may be considered that the glioma cells have little or less negatively regulating molecules for the MAPK pathway such as Ras-GAP but dominantly possess a positively regulating mechanism such as the enhancement of FGFR signaling by EphA4. From our results that ephrin-A1 stimulation alone did not affect the MAPK pathway, it is considered that the strength of these two negative and positive regulation may be different among the cell types, which may explain the discrepancy in the previous results regarding the regulation of the MAPK pathway by Eph receptors.

The FGFR-mediated phosphatidylinositol 3-kinase/Akt signaling pathway was also enhanced by EphA4, which was suggested by the findings that phospho-Akt was increased by EphA4 WT but inhibited by EphA4 DN (Fig. 3C). However, the Akt pathway was found to be activated by ephrin-A1 stimulation itself and to be inhibited by EphA4 DN. In addition, FGFR1 DN had no effect on the Akt pathway mediated by ephrin-A1 stimulation. This means that EphA4 has its own Akt activating pathway, except for the enhancement of FGFR-mediated Akt pathway in the U251 cells as reported that Akt pathway was mediated by Eph receptors (44).

Rho family GTPases are signaling molecules influencing cell motility by cytoskeletal reorganizing (46). Eph signaling modulates the balance of Rho versus Rac and Cdc42 activities (3, 6). As shown in Fig. 4, neither ephrin-A1 nor FGF2 changed the Rho activity of the U251 cells. The reason might be that the U251 glioma cells expressed little ephexin, a guanine nucleotide exchanging factor for Rho, which was identified as a direct signaling molecule relayed from EphA4 (data not shown; ref. 47). On the contrary, Rac1 and Cdc42 were both activated by FGF2 or ephrin-A1 stimulation and EphA4 further enhanced these activities. Interestingly, both Rac1 and Cdc42 activations were found to be inhibited by EphA4 DN and FGFR1 DN. This means that FGFR1 and EphA4 are both necessary to activate Rac1 and Cdc42 by either FGF2 or ephrin-A1 and a close functional association is suggested between their receptors. These results were consistent with the promoted migration by EphA4 shown in Fig. 4A and could explain why EphA4 enhanced the migration in the U251 cells. The contribution of other types of guanine nucleotide exchanging factors for Rac1 or Cdc42 might be important for the enhanced migration, but the precise mechanism remains to be elucidated.

As shown in Fig. 5, we clearly showed that EphA4 formed a complex with FGFR1 and FGFR1 activity was enhanced by EphA4. These results supported the reason why EphA4 enhanced FGFR-mediated MAPK, Akt pathway, and Rac1/Cdc42 activities. These findings were supported by the report showing the interaction between EphA4 and FGFR (32). This report also showed the direct association between two molecules and how they assembled to relay their signal. It is noteworthy that different types of receptor protein tyrosine kinases such as EphA4 and FGFR1 are able to interact with each other and enhance their functions. This means cross-talk between the receptors may exist at the plasma membrane and could produce a more diverse signaling mechanism in living cells. In the glioma cells, the EphA4-FGFR1 interaction is considered to promote proliferation and migration by acting as a enhancer for the malignant phenotype.

Long-term survival of patients with malignant gliomas has improved very little despite aggressive multimodality treatments including surgery, radiotherapy, and cytotoxic chemotherapy (48). One limitation of the conventional treatment is that these therapeutic strategies are not properly based on the malignant glioma-specific biological properties. Therefore, it is important to know the molecular-based characteristics (bioinformatics) of malignant gliomas to achieve a therapeutic breakthrough. Recently, the molecular targeting approach has been developed in treating many types of cancer (49). To realize the molecular targeting therapy in malignant gliomas, one strategy is to identify key molecules using the microarray technique (50). From this view, we analyzed gene expression in malignant gliomas using a DNA microarray and found high expression of EphA4 in malignant gliomas. We then clarified the functional significance of the overexpression of EphA4 using a human glioma cell line, U251 cells. Our collective results provide the typical strategy to analyze functionally the molecule that has been identified from the gene expression study. We expect EphA4-FGFR1 signaling may become a candidate as a potential target in therapeutic intervention for malignant gliomas and cell-based screening for an EphA4-specific inhibitor is ongoing based on our findings.

Disclosure of Potential Conflicts of Interest

No potential conflicts of interest were disclosed.

References

1. Murai KK, Pasquale EB. 'Eph'ective signaling: forward, reverse and crosstalk. J Cell Sci 2003;116:2823–32.

2. Eph Nomenclature Committee. Unified nomenclature for Eph family receptors and their ligands, the ephrins. Cell 1997;90:403–4.

3. Pasquale EB. Eph receptor signalling casts a wide net on cell behaviour. Nat Rev Mol Cell Biol 2005;6:462–75.

4. Pasquale EB. Eph-ephrin promiscuity is now crystal clear. Nat Neurosci 2004;7:417–8.

5. Henkemeyer M, Orioli D, Henderson JT, et al. Nuk controls pathfinding of commissural axons in the mammalian central nervous system. Cell 1996;86:35–46.

6. Kullander K, Croll SD, Zimmer M, et al. Ephrin-B3 is the midline barrier

that prevents corticospinal tract axons from recrossing, allowing for unilateral motor control. Genes Dev 2001;15:877–88.

7. Frisen J, Holmberg J, Barbacid M. Ephrins and their Eph receptors: multitalented directors of embryonic development. EMBO J 1999;18: 5159–65.

8. Lai KO, Ip FC, Cheung J, et al. Expression of Eph receptors in skeletal muscle and their localization at the neuromuscular junction. Mol Cell Neurosci 2001;17:1034–47.

9. Gerlai R. Eph receptors and neural plasticity. Nat Rev Neurosci 2001;2: 205–9.

10. Oike Y, Ito Y, Hamada K, et al. Regulation of vasculogenesis and angiogenesis by EphB/ephrin-B2 signaling between endothelial cells and surrounding mesenchymal cells. Blood 2002;100:1326–33.

11. Adams RH, Wilkinson GA, Weiss C, et al. Roles of ephrinB ligands and EphB receptors in cardiovascular development: demarcation of arterial/venous domains, vascular morphogenesis, and sprouting angiogenesis. Genes Dev 1999;13:295–306.

12. Easty DJ, Hill SP, Hsu MY, et al. Up-regulation of ephrin-A1 during melanoma progression. Int J Cancer 1999;84:494–501.

13. Vogt T, Stolz W, Welsh J, et al. Overexpression of Lerk-5/Eplg5 messenger RNA: a novel marker for increased tumorigenicity and metastatic potential in human malignant melanomas. Clin Cancer Res 1998;4:791–7.

14. Kiyokawa E, Takai S, Tanaka M, et al. Overexpression of ERK, an EPH family receptor protein tyrosine kinase, in various human tumors. Cancer Res 1994;54:3645–50.

15. Tang XX, Zhao H, Robinson ME, et al. Implications of EPHB6, EFNB2, and EFNB3 expressions in human neuroblastoma. Proc Natl Acad Sci U S A 2000;97:10936–41.

16. Walker-Daniels J, Coffman K, Azimi M, et al. Overexpression of the EphA2 tyrosine kinase in prostate cancer. Prostate 1999;41:275–80.

17. Miyazaki T, Kato H, Fukuchi M, et al. EphA2 overexpression correlates with poor prognosis in esophageal squamous cell carcinoma. Int J Cancer 2003;103:657–63.

18. Surawska H, Ma PC, Salgia R. The role of ephrins and Eph receptors in cancer. Cytokine Growth Factor Rev 2004;15:419–33.

19. Carles-Kinch K, Kilpatrick KE, Stewart JC, et al. Antibody targeting of the EphA2 tyrosine kinase inhibits malignant cell behavior. Cancer Res 2002;62:2840–7.

20. Nakada M, Niska JA, Miyamori H, et al. The phosphorylation of EphB2 receptor regulates migration and invasion of human glioma cells. Cancer Res 2004;64:3179–85.

21. Ornitz DM, Xu J, Colvin JS, et al. Receptor specificity of the fibroblast growth factor family. J Biol Chem 1996;271:15292–7.

22. Ong SH, Guy GR, Hadari YR, et al. FRS2 proteins recruit intracellular signaling pathways by binding to diverse targets on fibroblast growth factor and nerve growth factor receptors. Mol Cell Biol 2000;20:979–89.

23. Hadari YR, Kouhara H, Lax I, et al. Binding of Shp2 tyrosine phosphatase to FRS2 is essential for fibroblast growth factor-induced PC12 cell differentiation. Mol Cell Biol 1998;18:3966–73.

24. Schumacher S, Gryzik T, Tannebaum S, et al. The RhoGEF Pebble is required for cell shape changes during cell migration triggered by the *Drosophila* FGF receptor Heartless. Development 2004;131:2631–40.

25. Mohammadi M, Olsen SK, Ibrahimi OA. Structural basis for fibroblast growth factor receptor activation. Cytokine Growth Factor Rev 2005;16: 107–37.

26. Yamaguchi F, Saya H, Bruner JM, et al. Differential expression of two fibroblast growth factor-receptor genes is associated with malignant progression in human astrocytomas. Proc Natl Acad Sci U S A 1994;91: 484–8.

27. Morrison RS, Yamaguchi F, Saya H, et al. Basic fibroblast growth factor and fibroblast growth factor receptor I are implicated in the growth of human astrocytomas. J Neurooncol 1994;18:207–16.

28. Yamada SM, Yamaguchi F, Brown R, et al. Suppression of glioblastoma cell growth following antisense oligonucleotide-mediated inhibition of fibroblast growth factor receptor expression. Glia 1999;28: 66–76.

29. Kleihues P, Cavenee WK. WHO classification. Tumours of the nervous system. IARC Press; 2000. p. 27–39.

30. Yang YH, Dudoit S, Luu P, et al. Normalization for cDNA microarray data: a robust composite method addressing single and multiple slide systematic variation. Nucleic Acids Res 2002;30:e15.

31. Yamanaka R, Arao T, Yajima N, et al. Identification of expressed genes characterizing long-term survival in malignant glioma patients. Oncogene 2006;25:5994–6002.

32. Yokote H, Fujita K, Jing X, et al. Trans-activation of EphA4 and FGF receptors mediated by direct interactions between their cytoplasmic domains. Proc Natl Acad Sci U S A 2005;102:18866–71.

33. Wang W, Zhu NL, Chua J, et al. Retargeting of adenoviral vector using basic fibroblast growth factor ligand for malignant glioma gene therapy. J Neurosurg 2005;103:1058–66.

34. Bruce V, Olivieri G, Eickelberg O, et al. Functional activation of EphA5 receptor does not promote cell proliferation in the aberrant EphA5 expressing human glioblastoma U-118 MG cell line. Brain Res 1999; 821:169–76.

35. Nakada M, Niska JA, Tran NL, et al. EphB2/R-Ras signaling regulates glioma cell adhesion, growth, and invasion. Am J Pathol 2005;167:565–76.

36. Wykosky J, Gibo DM, Stanton C, et al. EphA2 as a novel molecular marker and target in glioblastoma multiforme. Mol Cancer Res 2005;3: 541–51.

37. Nakada M, Drake KL, Nakada S, et al. Ephrin-B3 ligand promotes glioma invasion through activation of Rac1. Cancer Res 2006;66: 8492–500.

38. Kullander K, Butt SJ, Lebret JM, et al. Role of EphA4 and EphrinB3 in local neuronal circuits that control walking. Science 2003;299:1889–92.

39. Iwasato T, Katoh H, Nishimaru H, et al. Rac-GAP α-chimerin regulates motor-circuit formation as a key mediator of EphrinB3/EphA4 forward signaling. Cell 2007;130:742–53.

40. Miao H, Wei BR, Peehl DM, et al. Activation of EphA receptor tyrosine kinase inhibits the Ras/MAPK pathway. Nat Cell Biol 2001;3:527–30.

41. Elowe S, Holland SJ, Kulkarni S, et al. Downregulation of the Ras-mitogen-activated protein kinase pathway by the EphB2 receptor tyrosine kinase is required for ephrin-induced neurite retraction. Mol Cell Biol 2001; 21:7429–41.

42. Kim I, Ryu YS, Kwak HJ, et al. EphB ligand, ephrinB2, suppresses the VEGF- and angiopoietin 1-induced Ras/mitogen-activated protein kinase pathway in venous endothelial cells. FASEB J 2002;16:1126–8.

43. Tong J, Elowe S, Nash P, et al. Manipulation of EphB2 regulatory motifs and SH2 binding sites switches MAPK signaling and biological activity. J Biol Chem 2003;278:6111–9.

44. Aoki M, Yamashita T, Tohyama M. EphA receptors direct the differentiation of mammalian neural precursor cells through a mitogen-activated protein kinase-dependent pathway. J Biol Chem 2004;279: 32643–50.

45. Vindis C, Cerretti DP, Daniel TO, et al. EphB1 recruits c-Src and p52Shc to activate MAPK/ERK and promote chemotaxis. J Cell Biol 2003; 162:661–71.

46. Etienne-Manneville S, Hall A. Rho GTPases in cell biology. Nature 2002;420:629–35.

47. Shamah SM, Lin MZ, Goldberg JL, et al. EphA receptors regulate growth cone dynamics through the novel guanine nucleotide exchange factor ephexin. Cell 2001;105:233–44.

48. Parney IF, Chang SM. Current chemotherapy for glioblastoma. Cancer J 2003;9:149–56.

49. Newton HB. Molecular neuro-oncology and development of targeted therapeutic strategies for brain tumors. Part 2. PI3K/Akt/PTEN, mTOR, SHH/PTCH and angiogenesis. Expert Rev Anticancer Ther 2004;4:105–28.

50. Korfee S, Gauler T, Hepp R, et al. New targeted treatments in lung cancer—overview of clinical trials. Lung Cancer 2004;45 Suppl 2: S199–208.

Establishment and molecular profiling of a novel human pancreatic cancer panel for 5-FU

Kazuyoshi Yanagihara,[1,4] Misato Takigahira,[1] Hiromi Tanaka,[1] Tokuzo Arao,[2] Yasuyuki Aoyagi,[3] Tatsuya Oda,[3] Atsushi Ochiai[3] and Kazuto Nishio[2]

[1]Central Animal Laboratory, National Cancer Center Research Institute, Tokyo, Tsukiji 5-1-1, Chuo-ku, Tokyo 104-0045; [2]Department of Genome Biology, Kinki University School of Medicine, Ohno-Higashi 377-2, Osaka-Sayama, Osaka 589-8511; [3]Pathology Division, Research Center for Innovative Oncology, National Cancer Center Research at Kashiwa, Kashiwanoha 6-5-1, Kashiwa, Chiba 277-8577, Japan

(Received April 30, 2008/Revised May 27, 2008/Accepted May 27, 2008/Online publication August 7, 2008)

Ten novel human pancreatic carcinoma cell lines (Sui65 through Sui74) were established from a transplantable pancreatic carcinoma cell line. All the cell lines resembled the original clinical carcinoma in terms of the morphological and biological features, presenting with genetic alterations such as point mutations of *K-ras* and *p53*, attenuation or lack of *SMAD4* and *p16* and other relevant cellular characteristics. Using this panel, we evaluated the effects of 5-FU in suppressing the proliferation of pancreatic carcinoma cells. When tested *in vitro*, although Sui72 was highly susceptible to 5-FU, the other cell lines were found to be resistant to the drug. When Sui72 and Sui70 were implanted subcutaneously in SCID mice followed by treatment with 5-FU, the drug was found to be effective against Sui72 but not Sui70, consistent with the results *in vitro*. In order to identify the molecular determinant for high sensitivity of Sui72 to 5-FU, we examined the mRNA expression levels of the metabolic enzymes of 5-FU. Decreased expression of DPYD was observed in Sui72 as compared with other cell lines (0.1 *versus* 0.6 ± 0.5, 0.1-fold).

It is believed that the novel cell lines established in the present study will be useful for analyzing the pattern of progression of pancreatic cancer and for evaluating the efficacy of anticancer agents. (*Cancer Sci* 2008; 99: 1859–1864)

Pancreatic cancer is an intractable cancer with a prognosis poorer than that of any other cancer of the gastrointestinal tract. In Japan, the 5-year survival rate of patients with pancreatic cancer is 5.5%, which is extremely low as compared with that of patients with colorectal cancer (64.6%), gastric cancer (58.8%) or even hepatic cancer (17.1%).[1,2] The number of patients with this cancer has been increasing significantly in recent years, and the mean life expectancy of patients with this cancer is only about 1.5 years. Pancreatic cancer, often characterized by pain, jaundice and digestive dysfunction, causes much pain and stress to the patient. These characteristics make this cancer an important open issue in medicine and healthcare. Currently, no valid clinical means are available for the prevention, diagnosis or treatment of this cancer. Treatment of pancreatic cancer with local therapy alone, that is surgical resection and radiotherapy, has limitations, and chemotherapy needs to be considered.[2] In the past, various adjuvant chemotherapy regimes, primarily based on 5-FU, have been attempted;[3–5] however, no effective therapy has as yet been established for pancreatic cancer.

In recent years, close attention has been paid to the development of cancer treatment methods based on information about the molecular mechanism of onset and progression of cancer.[2,6,7] Thus, exploration of molecular markers and target molecules for treatment is expected to play a key role in cancer management. For this kind of preclinical research, in particular, for evaluation of the efficacy of molecule-targeted drugs, the development of a panel of cultured cells derived from clinical cancer specimens is indispensable. To date, a number of cell lines derived from human pancreatic cancer have been established [8–15] and have contributed greatly to advancing cancer research[15,16] in terms of analysis of biological features and evaluation of the efficacy of anticancer agents. However, after multiple passages, some of these cell lines lose their original features (e.g. histopathological characteristics of the tumor formed after implantation, etc.).

The present study was undertaken to establish 10 novel cell lines derived from human pancreatic carcinoma that would reliably reflect the clinical features of pancreatic carcinoma. We investigated the proliferative characteristics and genetic alterations in these cell lines, then, using the panel of cell lines, we evaluated the efficacy of conventional 5-FU-based chemotherapy against pancreatic cancer and attempted to elucidate the determinants of sensitivity of these pancreatic cancer cell lines to 5-FU-based anticancer agents.

Materials and Methods

Establishment of the cell lines. All the cell lines were established *in vitro* from xenotransplantable tumors (taco series) originating from primary or metastatic human pancreatic cancer (Table 1) (T. Oda and A. Ochiai, unpublished data). The cell lines were established by s.c. back transplantation of the primary tumor for the 8th transplant generation, then tumors were removed for *in vitro* cultivation. Fresh tumor specimens obtained under sterile conditions were washed five times in Roswell Park Memorial Institute medium (RPMI)-1640 containing streptomycin (500 μg/mL) and penicillin (500 IU/mL). The tumor tissue specimens were trimmed of fat and necrotic materials and minced with a scalpel. The tissue pieces were transferred together with Dulbecco's Modified Eagle Medium (DMEM) + Ham's F12 + 5% fetal bovine serum (FBS), at 10–15 fragments per dish, to 60-mm culture dishes.[17] The dishes were left undisturbed for 24 h at 37°C in a 5% CO_2/95% air atmosphere. The medium was composed of Dulbecco's modified Eagle's medium (DMEM)/Ham's F12 medium (1:1) supplemented with 5% fetal bovine serum (FBS; Gibco, Grand Island, NY, USA), 100 IU/mL penicillin G sodium, and 100 mg/mL streptomycin sulfate (Immuno-Biological Laboratories [IBL], Fujioka, Japan). After 48 h, the medium was replaced by RPMI-1640 medium (IBL, Fujioka, Japan) supplemented with 10% FBS, 100 IU/mL penicillin G sodium and 100 mg/mL streptomycin sulfate. The dishes containing the tissue fragments were observed weekly under an inverted phase microscope. The dishes were initially trypsinized (0.05% trypsin and 0.02% ethylenediametetraacetic acid [EDTA]) to selectively remove overgrowing fibroblasts. In addition, we also attempted to remove the fibroblasts mechanically and transfer only the tumor cells. Half of the medium was changed every 4–6 days. The cultures were first split after 3–8 months of cultivation, and the

*To whom correspondence should be addressed. E-mail: kyanagih@ncc.go.jp
T. Oda and Y. Aoyagi are currently at HBP Surgery, Tsukuba University, Clinical Medicine, Japan.

Abbreviations: i.p., intraperitoneal; s.c., subcutaneous; TPA, tissue polypeptide antigen; 5-FU, 5-fluorouracil; SCID, severe combined immunodeficiency.

doi: 10.1111/j.1349-7006.2008.00896.x

Table 1. Establishment of ten human pancreatic cancer cell lines from the xenotransplantable tumors

Cell line	Source	Origin		Histology
	xenograft tumor	Age/sex	Source (TNM)	
Sui65	taco-1	63/F	Peritoneum (metastatic focus)	Tubular adenocarcinoma c/w meta
Sui66	taco-2	74/M	Pancreas	Tubular adenocarcinoma
Sui67	taco-4	73/F	Pancreas	Tubular adenocarcinoma
Sui68	taco-5	53/M	Pancreas	Adenocarcinoma
Sui69	taco-6	54/M	Pancreas	Tubular adenocarcinoma
Sui70	taco-7	53/M	Pancreas	Adenocarcinoma
Sui71	taco-12	65/M	Liver (metastatic focus)	Adenocarcinoma c/w meta
Sui72	taco-13	76/F	Pancreas	Tubular adenocarcinoma
Sui73	taco-15	65/F	Pancreas	Tubular adenocarcinoma
Sui74	taco-16	72/F	Pancreas	Adenocarcinoma

cells were passaged thereafter at a 1:10 or 1:20 ratio.[18] They were then judged, established and designated (Table 1). All of the cell lines were routinely tested for *Mycoplasma* using a PCR *Mycoplasma* Detection kit (Takara, Kyoto, Japan), and no contamination was detected. This study was conducted in accordance with the Declaration of Helsinki. Informed consent was obtained from all of the patients from whom the tumor specimens were obtained. The study protocol was approved by the institutional review board of the National Cancer Center (approved number: 17–43).

Animal experimentation. The animal experiment protocols were approved by the Committee for Ethics in Animal Experimentation, and the experiments were conducted in accordance with the Guideline for Animal Experiments of the National Cancer Center. Female SCID mice (C.B.17/Icr Jcl-scid) were purchased from CLEA Japan (Tokyo, Japan), and maintained under specific-pathogen-free conditions. Six- to 8-week-old mice were used for this experiment. The mice were housed in filter-protected cages and reared on sterile water. The ambient light was controlled to provide regular 12-h light : 12-h dark cycles.

Western blot analysis. *SMAD4* and *p16* expression was examined in all the cell lines using Western blotting.[19] An osteosarcoma (SaOs2) and a human embryonic kidney (293) cell line were used as positive controls for *p16* and *SMAD4*, respectively. Monoclonal mouse antihuman antibodies to *DPC4/Smad 4* (cloneB8, Santa Cruz Biotechnology, Santa Cruz, CA, USA) and to *p16* (clone G175-405, PharMingen, San Diego, CA, USA) were used.

Therapeutic studies with 5-fluorouracil (5-FU). S.C. implantation of 5×10^5 cultured cells suspended in 0.1 mL RPMI-1640 medium was conducted in 6-week-old female SCID mice. To evaluate the antitumor activity, 3 days after the tumor cell implantation, the mice were divided into three groups of six mice each according to the tumor volume on Day 0. The experimental mice were divided into a control group that received vehicle alone (saline), and experimental groups that received i.p. inoculation of different doses of the drug (50 and 100 mg/kg/head). On Days 3, 10 and 17, tumor-bearing mice received an i.p. injection of 5-FU. 5-FU was purchased from Sigma (St. Louis, MO, USA) and dissolved in saline before being injected. Tumor growth was measured weekly, in terms of the tumor diameter, with calipers. At appropriate intervals, or when moribund, the mice were sacrificed and the tissues were examined macroscopically for metastasis in various organs and then processed for histological examination, as described previously.[20]

Direct sequencing. Samples from the cell lines were analyzed for the presence of mutations in exon 1 of the K-*ras* (Kirsten rat sarcoma-2 viral oncogene homolog) gene and exons 5–8 of the p53 gene by direct sequencing of the PCR-amplified DNA fragments. PCR and direct sequencing were performed as described previously[21] using minor modifications.

Real-time reverse-transcription polymerase chain reaction. RNA derived from each cell line was converted to complementary DNA using a GeneAmp RNA PCR Core kit (Applied Biosystems, Foster City, CA, USA). Real-time reverse transcription–polymerase chain reaction (RT-PCR) were performed using Power SYBR Green PCR Master Mix (Applied Biosystems) and the 7900HT Fast Real-time PCR system (Applied Biosystems). The PCR conditions were as follows: one cycle of denaturation at 95°C for 10 min, followed by 40 cycles at 95°C for 15 s and 60°C for 60 s. Obtained data was normalized relative to glyceraldehyde-3-phosphate dehydrogenase (GAPD) expression. The following primers were used: DHFR-FW: 5′-GCA AAT AAA GTA GAC ATG GTC TGG A-3′; DHFR-RW: 5′-AGT TTA AGA TGG CCT GGG TGA-3′; FPGS-FW: 5′-TCT GCC CTA ACC TGA CAG AGG TG-3′; FPGS-RW: 5′-TCG TCC AGG TGG TTC CAG TG-3′; TP-FW: 5′-GAG GCA CCT TGG ATA AGC TGG A-3′; TP-RW: 5′-GCT GTC ACA TCT CTG GCT GCA TA-3′; UPP1-FW: 5′-GTA CTA TGC CCG GTG CTC CAA C-3′; UPP1-RW: 5′-CTC TGC CTT GAA GCA GGA ATC CA-3′; PRPS1-FW: 5′-AAC GCA TGC TTT GAG GCA GTA GTA G-3′; PRPS1-RW: 5′-CTG ATG GCT TCT GCA AGG ATC ATA-3′; DPYD-FW: 5′-CAA CGT AGA GCA AGT TGT GGC TAT G-3′; DPYD-RW: 5′-AGT CGA CAA TAG GGC AAA CAC TGA-3′; TYMS-FW: 5′-ATC ATC ATG TGC GCT TGG AAT C-3′; TYMS-RW: 5′-TGT TCA CCA CAT AGA ACT GGC AGA G-3′; OPRT-FW: 5′-CTG GCT CCC GAG TAA GCA TGA-3′; OPRT-RW: 5′-CTG CTG AGA TTA TGC CAC GAC CTA-3′; TK1-FW: 5′-ATT CTC GGG CCG ATG TTC TC-3′; TK1-RW: 5′-GCG AGT GTC TTT GGC ATA CTT GA-3′; MTHFR-FW: 5′-GGA CAC TAC CTC ACC TGC CAG TAT C-3′; MTHFR-RW: 5′-CCA GAA GCA GTT AGT TCT GAC ACC A-3′; NP-FW: 5′-CAA CCT ACC TGG TTT CAG TGG TCA-3′; NP-RW: 5′-CCG GTC GTA GGC ATC AGA CA-3′; UCK2-FW: 5′-TTC GTC AAG CCT GCC TTT GAG-3′; UCK2-RW: 5′-TGG ATG TGC TGC ACG ATG AG-3′; GAPD-FW: 5′-GCA CCG TCA AGG CTG AGA AC-3′; GAPD-RW: 5′-ATG GTG GTG AAG ACG CCA GT-3′.

Results

Establishment and characterization of pancreatic cancer cell lines. Ten cell lines derived from human pancreatic cancers (Sui65, Sui66, Sui67, Sui68, Sui69, Sui70, Sui71, Sui72, Sui73 and Sui74) were newly established in the present study (Table 1). All the cell lines formed mono-layered sheets with clustering on confluence (Fig. 1 upper column). These cell lines exhibited the typical morphologic features of epithelial cells, characterized by sheets of polygonal cells in a pavement-like arrangement. The Sui65, 67, 68, 70 and 71 cell lines were found to secrete carbohydrate antigen19-9 (CA19-9), the concentration of which in the culture supernatants varied from 69 to 450 units/mL (Table 2). Production of TPA was also detected from all of the cell lines. The doubling times of the cell lines varied from approximately 20.8 to 55.2 h in the RPMI-1640 medium

doi: 10.1111/j.1349-7006.2008.00896.x

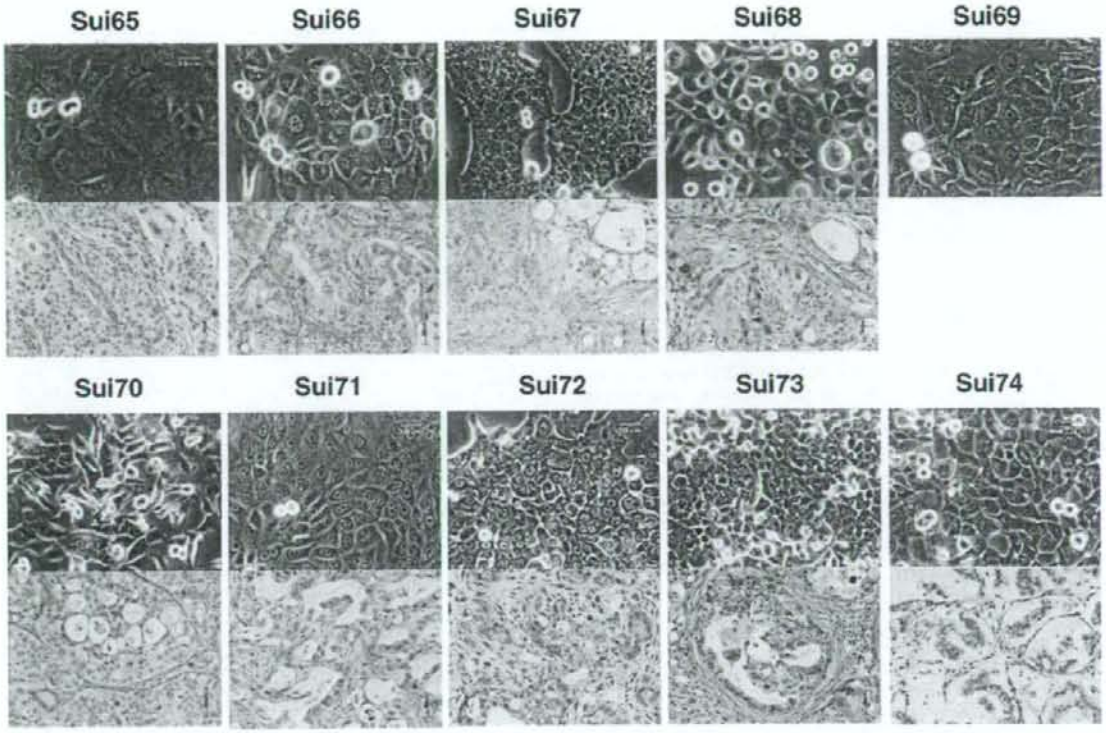

Fig. 1. Phase-contrast micrographs of the 10 established cell lines in this study (Sui65-Sui74) at the 25–30th passage (upper column). Original magnification, ×200. Histological section of a tumor established by s.c. injection of one of the cell lines into a SCID mouse (lower column). HE Stain, ×400.

Table 2. Biological characterization of newly established human pancreatic cancer cell lines

Cell line	Histological typing[1]		Growth[2]				Tumor marker[3]			
	Original	Xenografts	Pattern	in CDM	in Agar	DT (h)	CEA ng/mL	CA19-9 u/mL	TPA u/L	CA125 u/mL
Sui65	Tub.ad.	Mod.tub.ad.	M	+	+	48.6	<0.5	69	2600	32.2
Sui66	Tub.ad.	Mod./well.	M	+	+	41.2	1.2	<6	1800	2.2
Sui67	Tub.ad.	Poor.tub.ad.	M	+	+	35.1	2.6	420	1600	1.5
Sui68	Ad.	Poor./mod.	M	+	+	43.3	5.1	450	980	3.2
Sui69	Tub.ad.	(–)	M	–	–	55.2	0.6	<6	2200	<1.0
Sui70	Ad.	Mod.tub.ad.	M	+	+	20.8	<0.5	290	14 000	7.5
Sui71	Ad.	Well.tub.ad.	M	+	+	24.1	<0.5	170	7100	9.3
Sui72	Tub.ad.	Mod.tub.ad. Sarcoma	M	+	+	27.8	31.6	<6	4400	<1.0
Sui73	Tub.ad.	Well./mod.	M	+	+	23.5	<0.5	<6	2400	1.5
Sui74	Ad.	Mucinos ca.	M	+	+	47.5	<0.5	<6	1800	13.5

[1]The tumorigenicity of the cell lines were tested by s.c. injection of 5×10^6 cultured cells suspended in 0.1 mL RPMI-1640 medium into mice. Histological typing of the pancreatic cancer was conducted in accordance with the 'General Rules for the Study of Pancreatic Cancer (1993)', as tub (tubular adenocarcinoma), or Muci. ca. (Mucinous carcinoma).
[2]M, monolayer; CDM, composed of Dulbecco's modified Eagle's medium (DMEM)/Ham's F-12 (1:1) medium supplemented with 0.05% bovine serum albumin (BSA); +, positive; –, negative; DT, doubling time.
The doubling time of each line was determined as described previously.[20]
[3]Secretion of CEA, CA19-9, TPA and CA125 was tested by radioimmunoassay and immunoradioassay at SRL Laboratories (Tokyo, Japan).

supplemented with 10% FBS. When injected s.c., all of the cultured cell lines established from human pancreatic cancers, except for Sui69, survived and showed tumorigenicity (Fig. 1, lower column). These biological properties are summarized in Table 2. All the tumorigenic cell lines were also found to be strictly anchorage independent (60–90% efficiency).

Genetic alterations in the established pancreatic cancer cell lines. The results are summarized in Table 3. *K-ras* mutations were observed in eight of the 10 cell lines (80%). Activating mutations were detected in the 2nd base of codon 12 of *k-ras* in eight cell lines. The mutations were G-to-A transitions (GGT to GAT, Gly to Asp) in five cell lines, G-to-T transversions (GGT

Table 3. Molecular alterations of k-ras, p53, SMAD4 and P16 genes in newly established human pancreatic cancer cell lines

Cell line	Gene mutation				Gene expression	
	k-ras		p53		SMAD4/DPC4	p16
Sui65	codon12	GGT(Gly) → GAT(Asp)	codon248	CGG(Arg) → CAG(Gln)	–	–
Sui66	codon12	GGT(Gly) → GAT(Asp)	codon133	ATG(Met) → AAG(Lys)	+	–
Sui67	codon12	GGT(Gly) → GAT(Asp)	codon248	CGG(Arg) → TGG(Trp)	–	+
Sui68	codon12	GGT(Gly) → GAT(Asp)	codon245	GGC(Gly) → AGC(Ser)	+	–
Sui69	codon12	GGT(Gly) → GTT(Val)	codon175	CGC(Arg) → CAC(His)	–	–
Sui70	codon12	GGT(Gly) → GTT(Val)	codon175	CGC(Arg) → CAC(His)	–	–
Sui71	codon12	GGT(Gly) → GAT(Asp)	codon253	ACC(Thr) → CCC(Pro)	–	+
Sui72	Wt		codon135	TGC(Cys) → TAC(Tyr)	+	–
Sui73	Wt		Wt		+	–
Sui74	codon12	GGT(Gly) → CGT(Arg)	Wt	–	+	

to GTT, Gly to Val) in two cell lines and G-to-G transitions (GGT to GGT, Gly to Arg) in the remaining one cell line. Inactivating mutations of *p53* were found in eight of the 10 cell lines (80%), and included missense mutations.

Next, *SMAD4/DPC4* gene expression was checked by Western blot analysis. Marked expression of this gene was observed in Sui66 and Sui73, while the expression was less marked in Sui68 and Sui72; expression was altogether absent in the remaining six cell lines. Expression of the *P16* product was noted in Sui67, Sui71 and Sui74, but the levels were quite low or absent in the other cell lines (Table 3).

Therapeutic studies with 5-FU. Using this panel of human pancreatic cancer-derived cell lines, we evaluated the effect of 5-FU in suppressing the proliferation of each cell line *in vitro*. Sui69 was excluded from the analysis, since its proliferation rate was quite slow. The other nine cell lines were subjected to the MTT assay and the results are shown in Fig. 2. Sui72 was about 10-fold more susceptible to the drug, whereas the other cell lines were resistant to the drug.

Based on this result, we conducted a study *in vivo*, in which the highly drug-susceptible Sui72 and the resistant Sui70 were implanted subcutaneously in SCID mice. The 5-FU levels tested were 50 and 100 mg/kg/head. As shown in Fig. 3, tumor formation was markedly suppressed in all the mice implanted with Sui72. This suppressive effect was dose dependent, suggesting the effectiveness of 5-FU against this cell line. On the other hand, 5-FU did not inhibit the formation of tumor following implantation of Sui70, reflecting the findings *in vitro*.

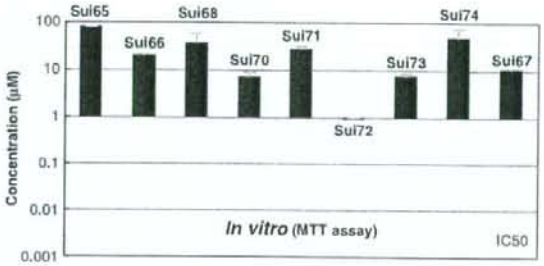

Fig. 2. Inhibition of growth of various human pancreatic cancer cell lines by 5-fluorouracil (5-FU) *in vitro*. The cell-growth inhibitory effects of 5-FU were assessed by the 3-(4,5-dimethylthiazol-2-yl)-2,5-diphenyltetrazolium bromide) (MTT) assay as described elsewhere.[21]

We attempted to identify the cause of the hypersensitivity of Sui72-5-FU by RT-PCR (Table 4). The mRNA expression levels of genes associated with the metabolisms of 5-FU, i.e. DHFR, EPGS, ECGF (TP), UPP1, PRPS1, TYMS (TS), UMPS (OPRT), TK1, MTHFR, NP (PNP) and UCK2 (UMPK) were analyzed in Sui72

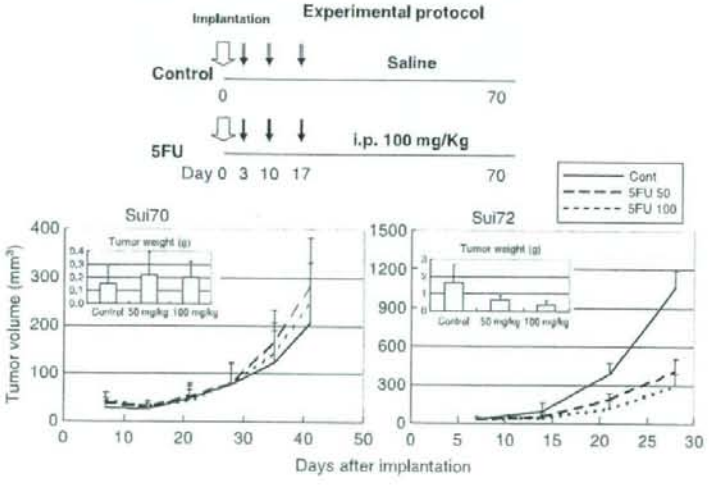

Fig. 3. Effect of 5-fluorouracil (5-FU) on Sui70 and Sui72 tumor growth in the SCID mouse. Six mice from each group were sacrificed when moribund, or on Day 28 or 40. The tumor mass was measured at predetermined time intervals in two dimensions with calipers, and the tumor volume was calculated according to the equation $(l \times w^2)/2$ [l = length, w = width].[18] Pancreatic carcinoma was confirmed by histopathology.

doi: 10.1111/j.1349-7006.2008.00896.x

Table 4. mRNA expression levels of genes related with 5-FU metabolism in a high sensitive Sui72 cells and in other human pancreatic cancer cell lines

Genes	Expression[†] The others[‡]	Expression[†] Sui72	Fold
DHFR	32.7 ± 37.8	33.1	1.0
FPGS	10.3 ± 18.3	n.d.	n.d.
TP	3.1 ± 4.6	0.1	0.0
UPP1	3.8 ± 5.0	1.6	0.4
PRPS1	9.1 ± 5.2	3.9	0.4
DPYD	0.6 ± 0.5	0.1	0.1
TYMS(TS)	49.9 ± 33.7	35.6	0.7
UMPS(OPRT)	7.2 ± 4.3	6.2	0.8
TK1	46.6 ± 46.3	28.4	0.6
MTHFR	4.4 ± 7.8	9.6	2.2
NP(PNP)	15.7 ± 8.0	23.3	1.5
UCK2(UMPK)	15.8 ± 9.7	29.7	1.9

n.d.: Not detectable by reverse transcription–polymerase chain reaction.
[†]Ratio of target gene/GAPD × 10-3 (fold).
[‡]The average ± SD of other cell lines except for Sui72.

as compared with other cell lines. Remarked decreased expression of DPYD was observed in Sui72 compared with other cell lines (0.6/–0.5). These results suggest that lower expression of DPYD is the molecular determinant of high sensitivity to 5-FU in Sui72 cells.

Discussion

A number of cultured cell lines have been established from human pancreatic cancers[8-14] and have contributed greatly to advancing cancer research by allowing biological characterization (analysis of the features of proliferation, progression, etc.) of this cancer and being useful as a preclinical research tool in the evaluation of anticancer agents.[15,16] However, after multiple passages, some of these cell lines lose their initial properties (e.g. the histopathological features of the tumors formed following their implantation). There seems to be a universal necessity for enriching the research resources through establishment of new cancer cell lines which would reliably reflect the clinical features of this cancer. Pancreatic cancer is usually characterized by stromal cell infiltration, therefore it is relatively difficult to establish pancreatic cancer cell lines.[16] Bearing this in mind, we first attempted to establish pancreatic cell lines from the tumors formed in SCID mice following implantation of primary or metastatic pancreatic cancer tissue. In this way, we established 10 cell lines of the Sui series. Half of the 10 cell lines were positive for the tumor marker CA19-9, while all were positive for TPA. The histopathological profile of most of the 10 cell lines resembled that of the original tumor. These findings indicate that the cell lines of this Sui series are pancreatic cancer cell lines reliably reflecting the clinical features of pancreatic cancer. However, one of these cell lines (Sui69) did not form a tumor in the SCID mice, even though it was transplantable. This Sui69 cell line exhibited very slow proliferative activity. We are currently studying this cell line in NOD-SCID or NOG mice.

Pancreatic cancer cells often exhibit genetic alternations. Point mutation of the oncogene *K-ras*, loss of heterozygosity (LOH; 9p, 17p, 18q, 1q, etc.), point mutation of tumor suppresser genes at these chromosomal locations (*p16*, *p53*, *DPC4/AMAD4*, etc.), methylation of the promoter region, etc., have been reported in pancreatic cancer.[22-25] Of the 10 cell lines established in this study, *K-ras* point mutation[26,27] and *p53* mutation[28] were noted in eight cell lines, and the genetic alterations found resembled those seen in the clinical materials. In Sui73, both *K-ras* and *p53* were wild type. The *SMAD4/DPC4* gene is known to show a high frequency of alterations (50%), including mutation (20%) and deletion (30%).[29,30] Marked expression of the *SMDA4/DPC4* gene was observed in two cell lines, and less marked expression in two cell lines; expression was altogether absent in the remaining six cell lines. Analysis of expression of the *P16/CDKN2A/INK4A* product in the 10 established cell lines revealed its expression in three cell lines, but the expression was quite low or altogether absent in remaining seven cell lines. It has been suggested that in pancreatic cancer free of *P16* mutations or deletions, expression of this gene is absent because of abnormal methylation of the gene expression–adjusting region and that most pancreatic cancers show malfunctioning of *P16*.[30,31] These changes are seen commonly in many cases of pancreatic cancer and seem to determine the proliferative potential and tumorigenicity of pancreatic cancer cells.

When treating pancreatic cancer, surgical resection, one or a various combination of surgical resection, systemic chemotherapy and radiotherapy is selected depending on the stage of the cancer.[2,25,32] Conventionally, various regimens of adjuvant chemotherapy, primarily involving 5-FU, have been attempted,[3-5] but no valid means of treating pancreatic cancer have yet been established. We attempted to evaluate the efficacy of 5-FU (a drug used as a standard therapy for this cancer in the past) against the cell lines established by us in this study. When tested *in vitro*, Sui72 was susceptible to the drug, whereas the remaining eight lines (Sui70, etc.) were found to be resistant to the drug. This finding was endorsed by the results of the *in vivo* study. We then explored the molecular determinant of sensitivity of the Sui72 cell line to 5-FU. The results of the analysis suggest that the decreased expression of DPYD may be involved in the mechanism of cellular sensitivity to 5-FU. In addition, decreased expression of TYMS was also observed in Sui72 as compared with other cell lines. This observation might be consistent with high sensitivity to 5-FU of Sui72 cells.

Throughout this study, it was shown that the new cell lines of the Sui series are useful for research on pancreatic cancer (e.g. evaluation of pancreatic cancer cell proliferation and progression, evaluation of the efficacy of anticancer agents, and so on).

New anticancer agents (e.g. TS-1, which reinforces the efficacy of 5-FU),[33-35] and gemcitabine hydrochloride (GEM) have recently become available for clinical use,[36-38] with the expectation of extending the survival period of patients with pancreatic cancer. To date, however, no chemotherapeutic agents more efficacious than GEM for pancreatic cancer have been developed. Clinical studies have therefore been carried out, focusing on developing treatment regimens containing GEM in combination with some other drugs. If GEM were combined with TS-1 or other molecule-targeted drugs, further extension of the survival period of pancreatic cancer patients may be expected. In the near future, we propose to carry out preclinical studies to evaluate the efficacy of various anticancer agents in SCID mice implanted with the new cell lines derived from human pancreatic cancer and to identify the genes, etc. which determine the susceptibility of pancreatic cancer cells to anticancer agents. It also seems to be essential to develop a model of orthotopic implantation, with the goal of establishing a drug evaluation system more relevant to the clinical setting.[25]

In conclusion, we established 10 cell lines derived from human pancreatic cancers that were found to possess biological characteristics and genetic alterations unique to pancreatic cancer. These new cell lines are expected to be highly useful for analyzing the pattern of pancreatic cancer progression and evaluating the efficacy of anticancer agents.

Acknowledgments

This study was supported in part by a Grant-in-Aid for Cancer Research from the Ministry of Health, Labour and Welfare of Japan. We are grateful to M. Namae and R. Nakanishi for their excellent technical work.

References

1 Tsukuma H, Ajiki W, Ioka A, Oshima A. Survival of cancer patients diagnosed between 1993 and 1996: a collaborative study of population-based cancer registries in Japan. *Jpn J Clin Oncol* 2006; **36**: 602–7. Epub 2006 Jul 26.

2 Okusaka T, Matsumura Y, Aoki K. New approaches for pancreatic cancer in Japan. *Cancer Chemother Pharmacol* 2004; **54**: S78–82.

3 Ikeda M, Okada S, Ueno H *et al.* A phase II study of sequential methotrexate and 5-fluorouracil in metastatic pancreatic cancer. *Hepatogastroenterology* 2000; **47**: 862–5.

4 Ueno H, Okada S, Okusaka T, Ikeda M, Kuriyama H. Phase II study of uracil-tegafur in patients with metastatic pancreatic cancer. *Oncology* 2002; **62**: 223–7.

5 Okada S. Non surgical treatments of pancreatic cancer. *Int J Clin Oncol* 1999; **4**: 257–66.

6 Bhattacharyya M, Lemoine NR. Gene therapy developments for pancreatic cancer. *Best Pract Res Clin Gastroenterol* 2006; **20**: 285–98.

7 Lohr JM. Medical treatment of pancreatic cancer. *Expert Rev Anticancer Ther* 2007; **7**: 533–44.

8 Kato M, Shimada Y, Tanaka H *et al.* Characterization of six cell lines established from human pancreatic adenocarcinomas. *Cancer* 1999; **85**: 832–40.

9 Ku JL, Yoon KA, Kim WH *et al.* Establishment and characterization of four human pancreatic carcinoma cell lines. Genetic alterations in the TGFBR2 gene but not in the MADH4 gene. *Cell Tissue Res* 2002; **308**: 205–14. Epub 2002 Apr 11.

10 Kawano K, Iwamura T, Yamanari H, Seo Y, Suganuma T, Chijiiwa K. Establishment and characterization of a novel human pancreatic cancer cell line (SUIT-4) metastasizing to lymph nodes and lungs in nude mice. *Oncology* 2004; **66**: 458–67.

11 Starr AN, Vexler A, Marmor S *et al.* Establishment and characterization of a pancreatic carcinoma cell line derived from malignant pleural effusion. *Oncology* 2005; **69**: 239–45. Epub 2005 Sept 2.

12 Sato N, Mizumoto K, Beppu K *et al.* Establishment of a new human pancreatic cancer cell line, NOR-P1, with high angiogenic activity and metastatic potential. *Cancer Lett* 2000; **155**: 153–61.

13 Mohammad RM, Li Y, Mohamed AN *et al.* Clonal preservation of human pancreatic cell line derived from primary pancreatic adenocarcinoma. *Pancreas* 1999; **19**: 353–61.

14 Kimura Y, Kobari M, Yusa T *et al.* Establishment of an experimental liver metastasis model by intraportal injection of a newly derived human pancreatic cancer cell line (KLM-1). *Int J Pancreatol* 1996; **20**: 43–50.

15 Ulrich AB, Schmied BM, Standop J, Schneider MB, Pour PM. Pancreatic cell lines: a review. *Pancreas* 2002; **24**: 111–20.

16 Iwamura T, Hollingsworth MA. Pancreatic tumors. In: Master JRW, Palsson B, eds. *Human Cell Culture*. Great Britain: Kluwer Academic Publishers, 1999; 107–22.

17 Yanagihara K, Tanaka H, Takigahira M *et al.* Establishment of two cell lines from human gastric scirrhous carcinoma that possess the potential to metastasize spontaneously in nude mice. *Cancer Sci* 2004; **95**: 575–82.

18 Yanagihara K, Takigahira M, Tanaka H *et al.* Development and biological analysis of peritoneal metastasis mouse models for human scirrhous stomach cancer. *Cancer Sci* 2005; **96**: 323–32.

19 Sun C, Yamato T, Furukawa T, Ohnishi Y, Kijima H, Horii A. Characterization of the mutations of the K-ras, p53, p16, and SMAD4 genes in 15 human pancreatic cancer cell lines. *Oncol Rep* 2001; **8**: 89–92.

20 Yanagihara K, Seyama T, Tsumuraya M, Kamada N, Yokoro K. Establishment and characterization of human signet ring cell gastric carcinoma cell lines with amplification of the c-myc oncogene. *Cancer Res* 1991; **51**: 381–6.

21 Arao T, Yanagihara K, Takigahira M *et al.* ZD6474 inhibits tumor growth and intraperitoneal dissemination in a highly metastatic orthotopic gastric cancer model. *Int J Cancer* 2006; **118**: 483–9.

22 Rozenblum E, Schutte M, Goggins M *et al.* Tumor-suppressive pathways in pancreatic carcinoma. *Cancer Res* 1997; **57**: 1731–4.

23 Loukopoulos P, Kanetaka K, Takamura M, Shibata T, Sakamoto M, Hirohashi S. Orthotopic transplantation models of pancreatic adenocarcinoma derived from cell lines and primary tumors and displaying varying metastatic activity. *Pancreas* 2004; **29**: 193–203.

24 Yatsuoka T, Sunamura M, Furukawa T *et al.* Association of poor prognosis with loss of 12q, 17p, and 18q, and concordant loss of 6q/17p and 12q/18q in human pancreatic ductal adenocarcinoma. *Am J Gastroenterol* 2000; **95**: 2080–5.

25 Giovannetti E, Mey V, Nannizzi S, Pasqualetti G, Del Tacca M, Danesi R. Pharmacogenetics of anticancer drug sensitivity in pancreatic cancer. *Mol Cancer Ther* 2006; **5**: 1387–95.

26 Almoguera C, Shibata D, Forrester K, Martin J, Arnheim N, Perucho M. Most human carcinomas of the exocrine pancreas contain mutant c-K-ras genes. *Cell* 1988; **53**: 549–54.

27 Hruban RH, van Mansfeld AD, Offerhaus GJ *et al.* K-ras oncogene activation in adenocarcinoma of the human pancreas. A study of 82 carcinomas using a combination of mutant-enriched polymerase chain reaction analysis and allele-specific oligonucleotide hybridization. *Am J Pathol* 1993; **143**: 545–54.

28 Redston MS, Caldas C, Seymour AB *et al.* p53 mutations in pancreatic carcinoma and evidence of common involvement of homocopolymer tracts in DNA microdeletions. *Cancer Res* 1994; **54**: 3025–33.

29 Hahn SA, Schutte M, Hoque AT *et al.* DPC4, a candidate tumor suppressor gene at human chromosome 18q21.1. *Science* 1996; **271**: 350–3.

30 Wilentz RE, Su GH, Dai JL *et al.* Immunohistochemical labeling for dpc4 mirrors genetic status in pancreatic adenocarcinomas: a new marker of DPC4 inactivation. *Am J Pathol* 2000; **156**: 37–43.

31 Caldas C, Hahn SA, da Costa LT *et al.* Frequent somatic mutations and homozygous deletions of the p16 (MTS1) gene in pancreatic adenocarcinoma. *Nat Genet* 1994; **8**: 27–32.

32 Hochster HS, Haller DG, de Gramont A *et al.* Consensus report of the international society of gastrointestinal oncology on therapeutic progress in advanced pancreatic cancer. *Cancer* 2006; **107**: 676–85.

33 Kaneko T, Goto S, Kato A *et al.* Efficacy of immuno-cell therapy in patients with advanced pancreatic cancer. *Anticancer Res* 2005; **25**: 3709–14.

34 Zhu AX, Clark JW, Ryan DP *et al.* Phase I and pharmacokinetic study of S-1 administered for 14 days in a 21-day cycle in patients with advanced upper gastrointestinal cancer. *Cancer Chemother Pharmacol* 2007; **59**: 285–93. Epub 2006 Jun 20.

35 Sakata Y, Ohtsu A, Horikoshi N, Sugimachi K, Mitachi Y, Taguchi T. Late phase II study of novel oral fluoropyrimidine anticancer drug S-1 (1 M tegafur-0.4 M gimestat-1 M otastat potassium) in advanced gastric cancer patients. *Eur J Cancer* 1998; **34**: 1715–20.

36 Rothenberg ML, Moore MJ, Cripps MC *et al.* A phase II trial of gemcitabine in patients with 5-FU-refractory pancreas cancer. *Ann Oncol* 1996; **7**: 347–53.

37 Burris HA, 3rd Moore MJ, Andersen J *et al.* Improvements in survival and clinical benefit with gemcitabine as first-line therapy for patients with advanced pancreas cancer: a randomized trial. *J Clin Oncol* 1997; **15**: 2403–13.

38 Aristu J, Canon R, Pardo F *et al.* Surgical resection after preoperative chemoradiotherapy benefits selected patients with unresectable pancreatic cancer. *Am J Clin Oncol* 2003; **26**: 30–6.

doi: 10.1111/j.1349-7006.2008.00896.x

Antitumor activity of cetuximab against malignant glioma cells overexpressing EGFR deletion mutant variant III

Junya Fukai,[1,2] Kazuto Nishio,[3] Toru Itakura[2] and Fumiaki Koizumi[1,4]

[1]Shien-Laboratory, National Cancer Center Hospital, Tsukiji 5-1-1, Chuo-ku, Tokyo, 104-0045; [2]Department of Neurological Surgery, Wakayama Medical University, Kimiidera 811-1, Wakayama, 641-0012; [3]Department of Genome Biology, Kinki University School of Medicine, Ohno-higashi 377-2, Osaka-sayama, Osaka, 589-8511, Japan

(Received February 22, 2008/Revised June 17, 2008/Accepted June 19, 2008/Online publication October 3, 2008)

Anti-epidermal growth factor receptor (EGFR) monoclonal antibody, cetuximab, is a promising targeted drug for EGFR-expressing tumors. Glioblastomas frequently overexpress EGFR including not only the wild type but also a deletion mutant form called 'variant III (vIII)', which lacks exon 2–7, does not bind to ligands, and is constitutively activated. In this study, we investigated the antitumor activity of cetuximab against malignant glioma cells overexpressing EGFRvIII. For this purpose, we transfected human malignant glioma cell lines with the retroviral vector containing cDNA for EGFRvIII, and analyzed the mode of cetuximab-induced action on the EGFRvIII in the cells. Immunoprecipitation and immunofluorescence revealed binding of cetuximab to EGFRvIII. Notably, immunoblotting analyses showed that cetuximab treatment resulted in reduced expression levels of the EGFRvIII. However, cetuximab alone did not exhibit a growth-inhibitory effect against the EGFRvIII-expressing cells. On the other hand, an assay for antibody-dependent cell-mediated cytotoxicity (ADCC) demonstrated cetuximab-induced cytolysis in the presence of human peripheral blood mononuclear cells in a dose-dependent manner. These results suggest that deletion mutant EGFRvIII can be a target of cetuximab and that ADCC activity substantially contributes to the antitumor efficacy of cetuximab against the EGFRvIII-expressing glioma cells. Thus, cetuximab could be a promising therapy in malignant gliomas that express EGFRvIII. (*Cancer Sci* 2008; 99: 2062–2069)

Long-term survival of patients with malignant gliomas has not substantially improved despite aggressive multimodality treatments including cytoreductive surgery, radiotherapy, and cytotoxic chemotherapy. To efficiently suppress these tumors, additional therapeutic strategies are necessary. Understanding the molecular genetics, biology, and immunology of gliomas will enable the potential development of new adjuvant treatments for malignant glioma patients.

Malignant gliomas may arise via a heterogeneous process resulting from multiple genetic alterations.[1] One of the well-known molecular features of gliomas is amplification of the epidermal growth factor receptor (*EGFR*) gene, leading to overexpression of this receptor in approximately 40–60% of glioblastomas.[2,3] High levels of EGFR expression have been shown to be correlated with malignant progression in gliomas and associated with a poor prognosis and resistance to therapies.[4] Therefore, therapeutic strategies directed against the EGFR may have potential in these malignancies.

In the EGFR-amplified tumors, multiple types of EGFR mutations can be detected as a result of intragene deletions.[2] The most frequent mutation in malignant gliomas is EGFR variant III (EGFRvIII), characterized by a consistent and tumor-specific in-frame deletion of 801 base pairs from the coding sequence of the extracellular domain.[5,6] This mutated gene encodes a protein with a ligand-independent and constitutively active tyrosine kinase domain, which greatly enhances the tumorigenicity of the cells, mostly found *in vivo*, not *in vitro*.[7–9] The deletion mutant EGFRvIII, which is clonally expressed on the cell surface of ~40% of glioblastomas, has been clinically correlated with increased glioma cell growth, proliferation, invasion, and angiogenesis.[2,10,11] For the EGFR-targeted strategies in malignant glioma therapy, EGFRvIII expression should be considered because of its highly malignant nature.

Methods of targeting the EGFR that have been developed and trialed include monoclonal antibodies (mAbs), synthetic tyrosine kinase inhibitors, conjugates of toxins to anti-EGFR mAbs and ligands, and antisense gene therapy of EGFR.[12,13] Small molecule tyrosine kinase inhibitors and mAbs are the most fully developed of these approaches.[14,15]

Cetuximab (Erbitux, IMC-C225) is a recombinant, human-murine chimeric mAb specifically targeting the EGFR.[13] Cetuximab competes with endogenous ligands for binding to the extracelluar domain of EGFR and binding of cetuximab prevents stimulation of the receptor by ligands. Cetuximab-binding also results in internalization of the antibody-receptor complex which leads to down-regulation of EGFR expression on the cell surface.[13] Furthermore, this type of mAb including the human IgG1 Fc region may cause recruitment and activation of host immune-effector cells (T cells, natural-killer cells, and macrophages) or complements to induce antibody-dependent cell-mediated cytotoxicity (ADCC) or complement-dependent cytotoxicity (CDC).[16,17]

A variety of human epithelial cancers expressing EGFR have been successfully treated by cetuximab with promising results and it was recently approved for use in treating advanced-stage EGFR-expressing colorectal, head, and neck cancers.[13,18] However, little is known as to whether or not it is an effective therapy for the treatment of highly malignant tumors expressing deletion mutant EGFRvIII. Based on the encouraging results of cetuximab in the EGFR-expressing cancers and the importance of EGFRvIII expression in the biology of glioblastomas, we investigated whether cetuximab would be capable of effectively targeting the EGFRvIII expressed in malignant glioma cell lines.

Materials and Methods

Cell culture. Human glioblastoma cell lines were obtained as follows: U-251 MG, A-172, SF126, and YH-13, JCRB Cell Bank (Osaka, Japan); U-118 MG, U-87 MG, DBTRG-05 MG, LN-229,

[4]To whom correspondence should be addressed.
E-mail: fkoizumi@gan2.res.ncc.go.jp

doi: 10.1111/j.1349-7006.2008.00945.x

LN-18, and M059K, ATCC (Manassas, VA, USA). These cell lines were maintained in RPMI-1640 supplemented with 10% fetal bovine serum and cultured at 37°C in a humidified atmosphere containing 5% CO_2.

Expression vector construction and cell transfection. Construction of expression vector was generously contributed by Dr Hideyuki Yokote (Wakayama, Japan). Full-length cDNA of wild-type (wt) EGFR was amplified by reverse transcription–polymerase chain reaction (RT-PCR) from a human embryonal kidney cell line HEK293 using a High Fidelity RNA PCR Kit (TaKaRa, Shiga, Japan) and the following primer sets: forward, CGCTAGCGATGCGACCCTCCGGGAC; reverse, CCCCTGACTCCGTCCAGTATTGA. The PCR products were amplified using the following primer sets: forward, CGCTAGCGATGCGACCCTCCGGGAC; reverse, CGAAGCTTTGCTCCAATAAATTCACTGC. The amplified DNA included NheI- and HindIII-cut cohesive ends at the 5′- and 3′-ends, respectively. The product was subcloned into a pCR BluntII-TOPO vector (Invitrogen, Carlsbad, CA, USA) and the sequences were confirmed. Oligonucleotides encoding the myc-tag sequence (EQKLISEEDLN) were designed and synthesized as follows: forward, AGCTTGAACAGAAGCTGATCTCAGAGGAGGACCTGAATTGAC; reverse, TCGAGTCAATTCAGGTCCTCCTCTGAGATCAGCTTCTGTTCA. These oligos were annealed, and the ds-oligos were generated including HindIII- and XhoI-cut cohesive ends, at the 5′- and 3′-ends, respectively. Wt EGFR and myc-tag DNA fragments were cut out and transferred into a pQCXIX retroviral vector (BD Biosciences Clontech, San Diego, CA, USA) containing EGFP following internal ribosome entry site sequence. EGFRvIII was synthesized with the recombinant PCR method using the following primers: F1, CGCTAGCGATGCGACCCTCCGGGAC; R1, ATCTGTCACCACATAATTACCTTTCTTTTCCTCCAGAGCC; F2, GGCTCTGGAGGAAAAGAAAGGTAATTATGTGGTGACAGAT; R2, CGGTGGAGGTGAGGCAGATG. Two DNA fragments of wt EGFR were amplified using the F1/R1 and F2/R2 primer sets. The EGFR fragment deleting exon 2–7 was amplified using the two PCR products as templates and the F1/R2 primer set. After confirming the sequence, a wt EGFR fragment was substituted for the NheI- and EcoRI- cut recombinant PCR fragment. A pVSV-G vector (BD Biosciences Clontech) and the pQCXIX constructs were cotransfected into the GP2-293 cells (BD Biosciences Clontech) using a FuGENE6 transfection reagent (Roche Diagnostics, Basel, Switzerland). Briefly, 80% confluent cells cultured on a 10-cm dish were transfected with 2-mg pVSV-G plus 6-mg pQCXIX vectors. Forty-eight h after transfection, culture medium was collected and the viral particles were concentrated by centrifugation. The viral pellet was resuspended in fresh medium. The titer of the viral vector was calculated by counting the EGFP-positive cells which were infected by serial dilution of the virus-containing medium and the multiplicity of infection was determined.

Chemicals. Cetuximab was kindly provided by Brystol-Myers Squibb (Princeton, NJ, USA).

Antibodies. Abs were purchased as follows: antihuman EGFR mouse mAb cocktail, Biosource Corp. (Camarillo, CA, USA); antiphosphotyrosine mouse mAb, BD Biosciences; antiphospho-Akt, phospho-p44/42 mitogen activated protein kinase (MAPK), rabbit polyclonal, anti-β-actin rabbit monoclonal, and antimouse and rabbit IgG horseradish peroxidase–linked Abs, Cell Signaling Technology (Beverly, MA, USA).

Immunoblotting. Cells were seeded and grown to near confluency. Then, cells were washed with phosphate-buffered saline (PBS) and culture medium with or without cetuximab was added. At the time of harvest, cells were washed and lyzed with lysis buffer (50 mM Hepes buffer, 1% Triton X-100, 5 mM ethylenediaminetetraacetic acid [EDTA], 50 mM sodium chloride, 10 mM sodium pyrophosphate, 50 mM sodium fluoride, and 1 mM sodium orthovanadate) supplemented with protease inhibitors (Roche Diagnostics, Penzberg, Germany). Cell lysates were clarified by centrifugation, and equal concentrations of lysates were mixed with 4× sodium dodecyl sulfate (SDS)–gel sample buffer (0.25 mol/L Tris-HCl, pH 6.8, 2% SDS, and 25% glycerol), denatured with 2-mercaptoethanol. Equivalent amounts of protein were separated on SDS-polyacrylamide gels by electrophoresis, and transferred onto polyvinylidene difluoride (PVDF) membranes by wet electroblotting. The PVDF membranes were blocked with 3% bovine serum albumin in PBS with 0.1% Tween-20 and probed with primary Ab. The membranes were washed and incubated with secondary Ab. After the membranes were washed, immunoblotted proteins were detected using the ECL Western Blotting Detection System (GE Healthcare, Buckinghamshire, UK).

Immunoprecipitation. Cell lysates were extracted and treated with Ab overnight at 4°C. The lysates were mixed with protein A agarose and centrifuged. Immunoprecipitates were washed with lysis buffer and resuspended in 1.5× SDS-sample buffer and denatured with 2-mercaptoethanol. Samples were processed by immunoblotting.

Immunofluorescence. For immunofluorescence, cells were grown overnight, washed in PBS and fixed for 20 min in 4% paraformaldehyde at room temperature (RT). Cells were then washed twice in PBS and blocked for 1 h in 10% normal goat serum at RT. Cetuximab (10 mg/mL) was diluted in 1.5% normal goat serum and incubated overnight at 4°C. Cells were washed twice in PBS for 5 min and incubated with a secondary Ab for 45 min at RT. Secondary Abs included Alexa Fluor 546 Goat Anti-Mouse IgG (2 mg/mL; Molecular Probes, Invitrogen) and Texas Red antihuman IgG (1.5 mg/mL; Vector, Burlingame, CA, USA). Cells were washed twice for 5 min in PBS and then examined under a microscope (Keyence Biozero, Osaka, Japan).

Growth-inhibition assay (MTS assay). The growth-inhibitory effect of cetuximab was evaluated using the CellTiter96 Aqueous One Solution Cell Proliferation Assay (Promega Corporation, Madison, WI, USA). MTS (3-[4,5-dimethylthiazol-2-yl]-5-[3-carboxymethoxyphenyl]-2-[4-sulfophenyl]-2H-tetrazolium, inner salt) provides a measure of mitochondrial dehydrogenase activity within the cell and thereby offers an indication of cellular proliferation status.[19] Briefly, 3000 cells were seeded in 96-well plates. The plates were incubated overnight to permit adherence. Cells were then exposed to different concentrations of cetuximab ranging from 0 to 100 mg/mL for 48 h. MTS reagent was added and incubated for 1 h. The plates were read on a microplate spectrophotometer (optical density, 490 nm). The percentage cell growth was calculated by comparison of the absorbance value reading obtained from treated samples *versus* controls.

Antibody-dependent cell-mediated cytotoxicity (ADCC). Peripheral blood mononuclear cells (PBMCs) were separated from whole blood of healthy volunteers using LSM Lymphocyte Separation Medium (Cappel, Aurora, OH, USA). 1×10^5 cells were seeded into each well of a 12-well plate. After incubation for 24 h, human PBMCs alone (effector : target = 10:1), and/or cetuximab (10 mg/mL), control human IgG (10 mg/mL), or control medium were added to the wells. The cultures were then examined under a microscope (Keyence) 24-h post treatment.

Propidium iodide (PI) nucleic acid stain for cetuximab-mediated ADCC. This assay was performed for identifying dead cells in a population under the same experimental condition as described in the 'ADCC' section. A 4-μM solution of Cellstain PI (1 mg/mL; Dojindo, Kumamoto, Japan) was made at a dilution rate of 1:3000 and added per well. After incubation in the dark for 15 min, cells were viewed under a microscope (Keyence).

MTS assay for cetuximab-mediated ADCC. For analysis of the ADCC activity of cetuximab, we used the MTS assay.[20] Briefly, 3000 cells per well were exposed to various concentrations of cetuximab in the presence of PBMCs at an effector/target (E/T) ratio of 10 for 48 h. Natural killer (NK) activity was calculated from the absorbance value of the cells cultured without cetuximab

and PBMCs (A), the absorbance value of the cells cultured with PBMCs (B), the absorbance value of medium alone (C), and the absorbance value of PBMCs (D) as follows: $\{1 - [(B - C) - (D - C)]/[(A - C) - (D - C)]\} \times 100$. ADCC was calculated from the values of A, D, the NK activity (E), and the absorbance value of the cells treated with cetuximab and PBMCs (F): $\{1 - (F - D)/(A - D)\} \times 100 - E$.

Results

Initially, we determined the expression of endogenous EGFR protein in 10 human malignant glioma cell lines by immunoblotting (Fig. 1a). All of these malignant glioma cell lines displayed only low amounts of wt EGFR protein (170 kDa) but not EGFRvIII protein (145 kDa). These findings were consistent with the previous notion that because primary explants of human glioblastoma rapidly lose expression of amplified, rearranged receptors in culture, no existing glioblastoma cell lines exhibit such expression.[22] Therefore, we introduced the *EGFRvIII* gene into malignant glioma cell lines and engineered them to express this mutant receptor protein in three cell lines: U-251 MG, U-87 MG, and LN-229 (Fig. 1b). Malignant glioma cells that expressed the EGFRvIII protein were observed under fluorescence microscopy due to the coexpression of EGFP (Fig. 1c).

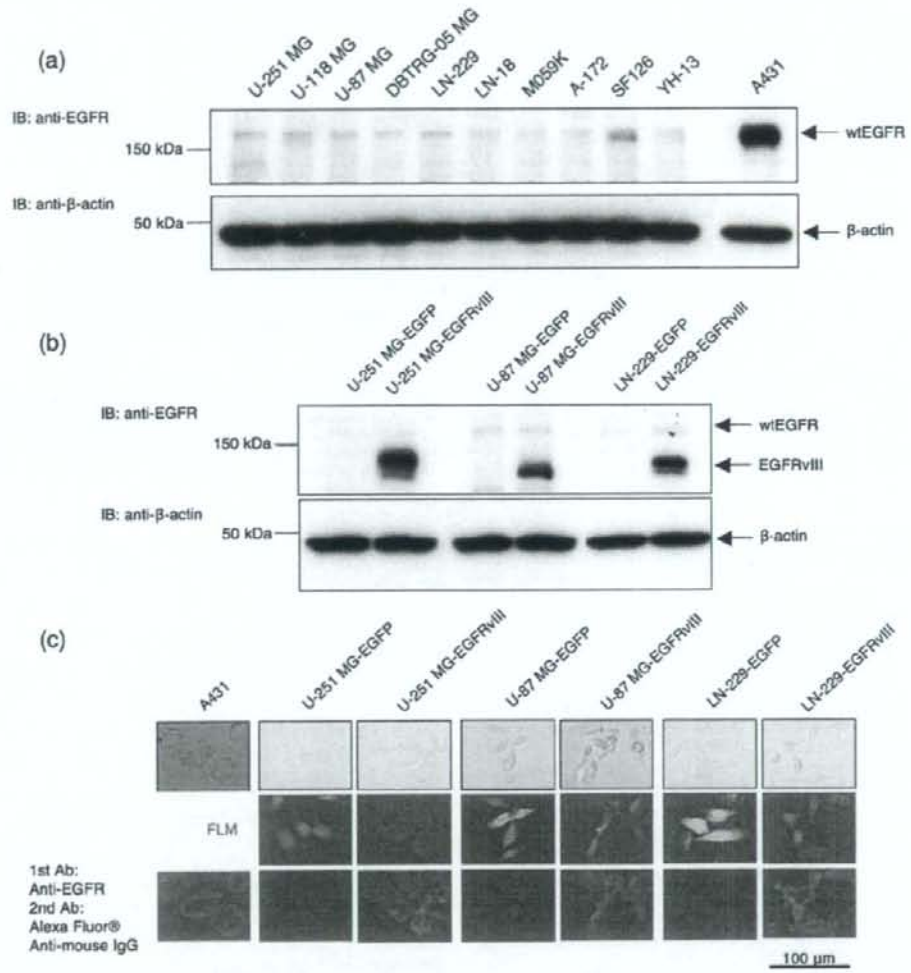

Fig. 1. (a) Expression of epidermal growth factor receptor (EGFR) in human malignant glioma cell lines. Ten malignant glioma cell lines were cultured and lyzed. Equal amounts of cell lysate were immunoblotted with anti-EGFR antibody (Ab) to show endogenous expression of EGFR. The human epidermoid carcinoma A431 cell lines served as a reference marker for high expression of wild-type (wt) EGFR.[21] Beta-actin showed protein loading. IB, immunoblotting. (b) Introduction of EGFRvIII into human malignant glioma cell lines. Three malignant glioma cell lines, into which the *EGFRvIII* gene was introduced, were cultured and lyzed. Equal amounts of cell lysates were immunoblotted with an anti-EGFR Ab to recognize exogenous expression of EGFRvIII. (c) Microscopic images and immunofluorescence of malignant glioma cells expressing EGFRvIII. EGFRvIII-expressing cells (*EGFRvIII*) were monitored by their coexpression of EGFP. Mock control (*EGFP*) expressed only EGFP. FM, fluorescent microscopy. EGFRvIII-expressing cells were stained with anti-EGFR Ab, then Alexa Fluor-conjugated antimouse IgG secondary Ab (lower panels). Staining of A431 or *EGFP* served as a reference of endogeneously expressed wt EGFR. Scale bar represents 100 μm.

doi: 10.1111/j.1349-7006.2008.00945.x

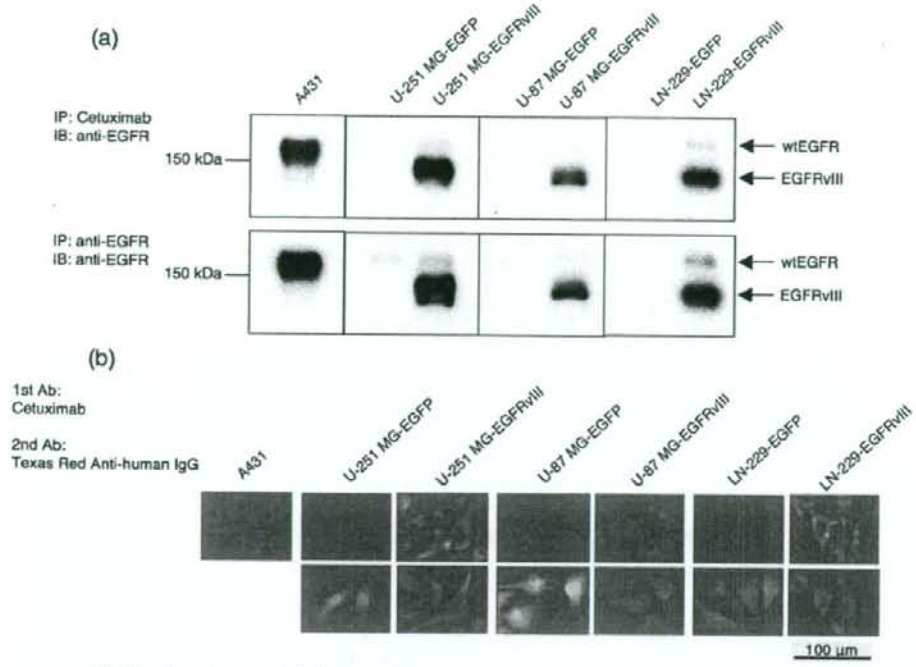

Fig. 2. (a) Immunoprecipitation showing cetuximab binding to epidermal growth factor receptor variant III (EGFRvIII). EGFRvIII-expressing cells were washed and lyzed. Equal amounts of cell lysates were immunoprecipitated with cetuximab or anti-EGFR antibody (Ab). The immunoprecipitates were probed by immunoblotting with anti-EGFR Ab. *A431* was used as a positive control for wild-type (wt) EGFR expression, and *EGFP* as a negative control for EGFRvIII. (b) Immunofluorescence showing cetuximab reactivity with malignant glioma cells expressing EGFRvIII. EGFRvIII-expressing cells were stained with cetuximab, then Texas Red–conjugated antihuman IgG secondary Ab. Staining of A431 or *EGFP* served as a reference for cetuximab reactivity with endogeneously expressed wt EGFR. Scale bar represents 100 μm.

Cetuximab has a binding ability to EGFRvIII. We investigated the binding capability of cetuximab to EGFRvIII by immunoprecipitation. Cell lysates were precipitated with cetuximab and then analyzed by immunoblotting with an anti-EGFR Ab. Cetuximab was found to precipitate the 140-kDa EGFRvIII protein from the EGFRvIII-expressing cells (Fig. 2a upper lane). There was no indication of an immunoreactive band migrating at the expected size of EGFRvIII in the mock control. The finding that the EGFRvIII protein was immunoprecipitated with cetuximab was confirmed by anti-EGFR Ab recognizing this mutant receptor (Fig. 2a lower lane).

Next, we performed immunofluorescence to investigate cetuximab reactivity with the EGFRvIII-overexpressing glioma cells. In this assay, cetuximab was used as a primary Ab, and Texas Red–conjugated antihuman IgG as a secondary Ab. In the mock control expressing low amounts of wt EGFR, we observed very low levels of staining, most of which were close to the detection limit of the analysis (Fig. 2b). In contrast, strong staining was evident in the EGFRvIII-overexpressing cells. Together these results demonstrate that cetuximab could recognize the deletion mutant EGFRvIII.

Cetuximab attenuates EGFRvIII expression and reduces phosphorylated EGFRvIII, but does not significantly inhibit Akt and MAPK signaling pathways. Based on the previous report that cetuximab-binding leads to down-regulation of EGFR expression, we investigated the effect of cetuximab on EGFRvIII expression by immunoblotting.[13] On treatment with cetuximab at various concentrations, the expression levels of EGFRvIII protein decreased dramatically in a dose-dependent manner (data not shown and Fig. 3a lower lane). In addition, we assessed the phosphorylation status of EGFRvIII by immunoprecipitation from the same lysates using a mAb recognizing EGFRvIII. The amount of immunoprecipitated EGFRvIII is shown in Fig. 3(a) (lower lane). A dose-dependent decrease in the expression of phosphorylated EGFRvIII was also observed, and the levels of tyrosine-phosphorylation corresponded to the expression of this receptor (Fig. 3a upper lane). Neither higher concentrations of cetuximab (= 100 μg/mL) nor prolonged exposure (72 h) augmented the effects on phosphorylated EGFRvIII expression (Fig. 3b and data not shown). Thus, cetuximab appeared to attenuate the EGFRvIII expression and reduce the phosphorylated EGFRvIII.

Next, we examined the phosphorylation status of Akt and MAPK pathways. On treatment with cetuximab, phosphorylated Akt and MAPK mildly decreased in the cells at higher concentrations (Fig. 3b). The decreased levels were not so significant as that of phosphorylated EGFRvIII. In summary, these results would suggest that when treated with cetuximab, EGFRvIII expression was markedly attenuated, while its downstream pathways by Akt and MAPK remained activated in the EGFRvIII-overexpressing glioma cells.

Cetuximab does not inhibit the growth of EGFRvIII-overexpressing glioma cells. We examined the effects of cetuximab on the growth of EGFRvIII-overexpressing glioma cells with an MTS assay. As can be observed in Fig. 4, cetuximab treatment did not produce a clear growth-inhibitory effect in the EGFRvIII-overexpressing cells even at the highest concentration tested. Also, treatment with cetuximab had a modest effect on the mock control. These data might support the findings determined by immunoblotting analyses.